

## Electronic Supplementary Information

### DNA and BSA Binding, Anticancer and Antimicrobial Properties of Co(II), Co(II/III), Cu(II) and Ag(I) Complexes of Arylhydrazones of Barbituric Acid

Jessica Palmucci,<sup>a,b</sup> Kamran T. Mahmudov,<sup>a,c,\*</sup> M. Fátima C. Guedes da Silva,<sup>a,\*</sup>  
Fabio Marchetti,<sup>b</sup> Claudio Pettinari,<sup>d</sup> Dezemona Petrelli,<sup>e</sup> Luca A. Vitali,<sup>f</sup> Luana Quassinti,<sup>f</sup>  
Massimo Bramucci,<sup>d</sup> Giulio Lupidi,<sup>f,\*</sup> Armando J. L. Pombeiro<sup>a,\*</sup>

<sup>a</sup> Centro de Química Estrutural, Instituto Superior Técnico, Universidade de Lisboa, Av. Rovisco Pais, 1049–001 Lisbon, Portugal

<sup>b</sup> School of Science and Technology, University of Camerino, Chemistry Section, via S. Agostino 1, 62032 Camerino, Italy

<sup>c</sup> Department of Chemistry, Baku State University, Z. Xalilov Str. 23, Az 1148 Baku, Azerbaijan

<sup>d</sup> School of Pharmacy, University of Camerino, Chemistry Section, via S. Agostino 1, 62032 Camerino, Italy

<sup>e</sup> School of Biosciences and Veterinary Medicine, University of Camerino, Piazza dei Costanti 4, 62032 Camerino, Italy

<sup>f</sup> School of Pharmacy, University of Camerino, Biological Section, via Gentile III da Varano, 62032 Camerino, Italy

\*Corresponding authors

*E-mail addresses:*

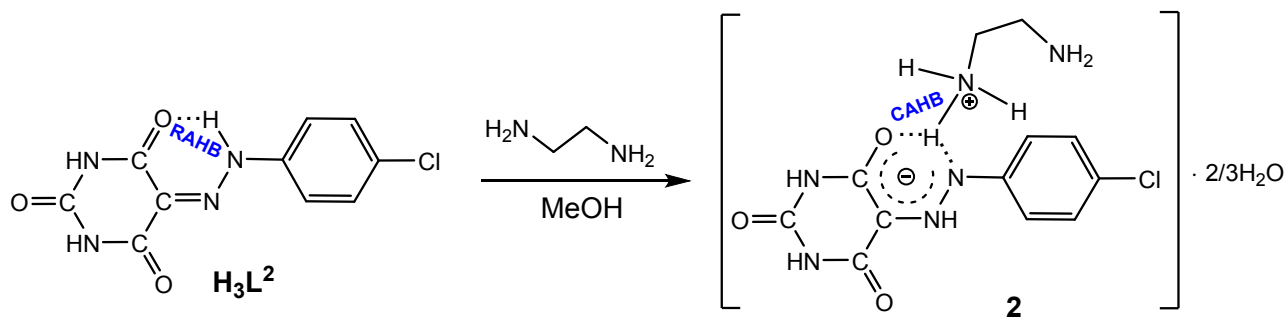
[kamran\\_chem@mail.ru](mailto:kamran_chem@mail.ru), [kamran\\_chem@yahoo.com](mailto:kamran_chem@yahoo.com) (Kamran T. Mahmudov)

[fatima.guedes@tecnico.ulisboa.pt](mailto:fatima.guedes@tecnico.ulisboa.pt) (M. Fátima C. Guedes da Silva)

[giulio.lupidi@unicam.it](mailto:giulio.lupidi@unicam.it) (Giulio Lupidi)

[pombeiro@tecnico.ulisboa.pt](mailto:pombeiro@tecnico.ulisboa.pt) (Armando J. L. Pombeiro)

## 1. Synthesis of 2



Scheme 1S. RAHB to CAHB transformations in the synthesis of **2**.

## 2. NMR and IR spectra of $H_3L^2$ , **1**, **2**, **7** and **8**.

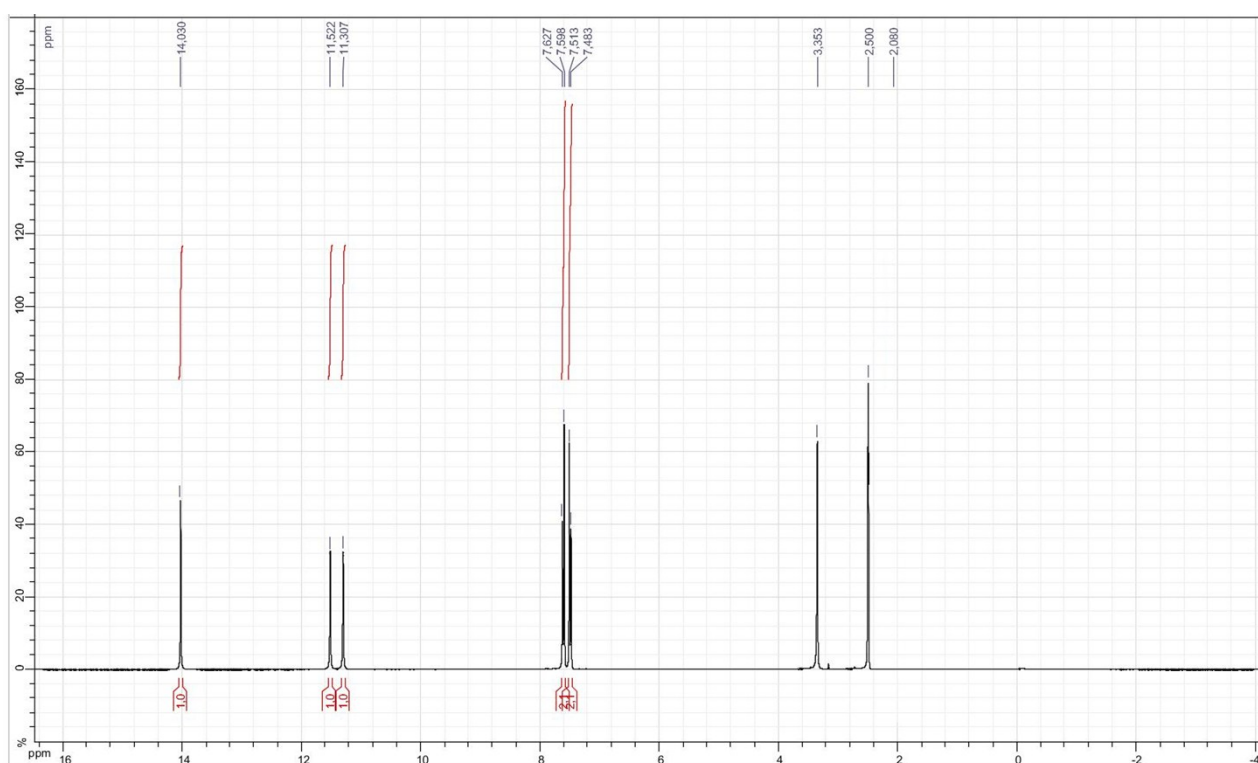


Figure 1S.  $^1H$  NMR spectra of  $H_3L^2$ .

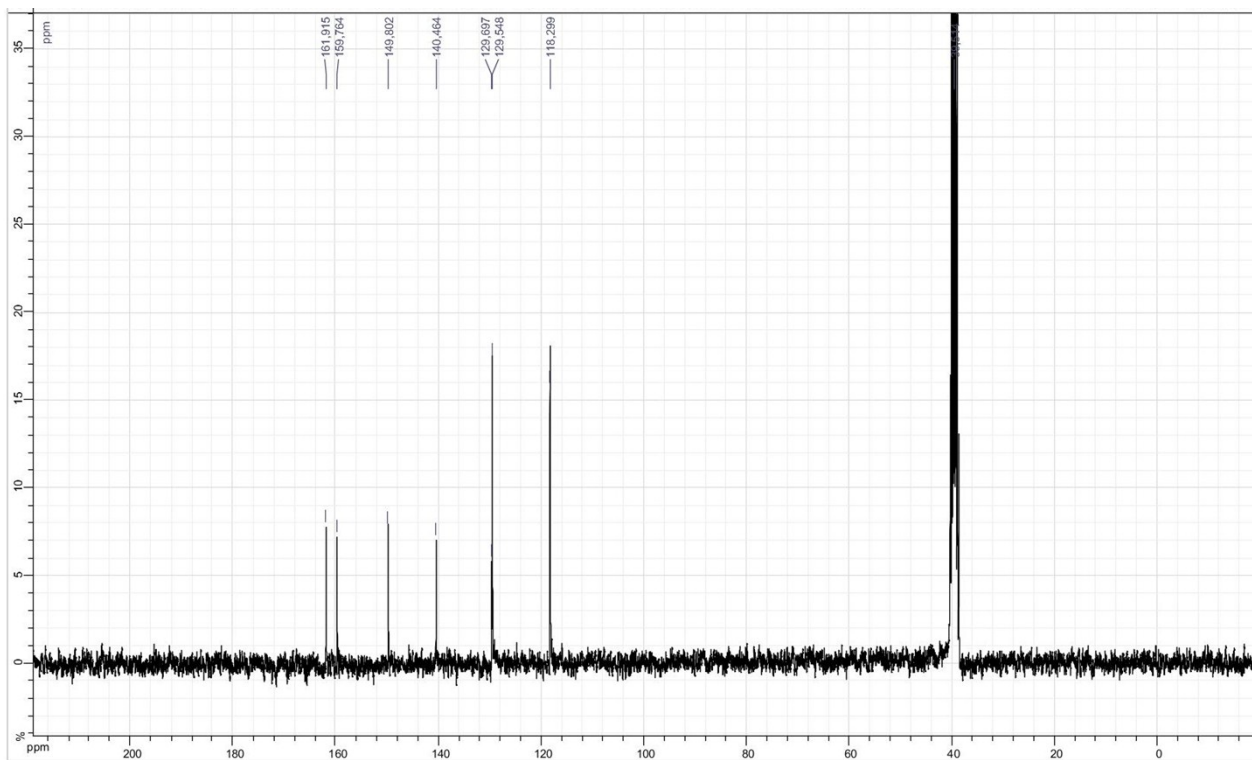


Figure 2S. <sup>13</sup>C NMR spectra of H<sub>3</sub>L<sup>2</sup>.

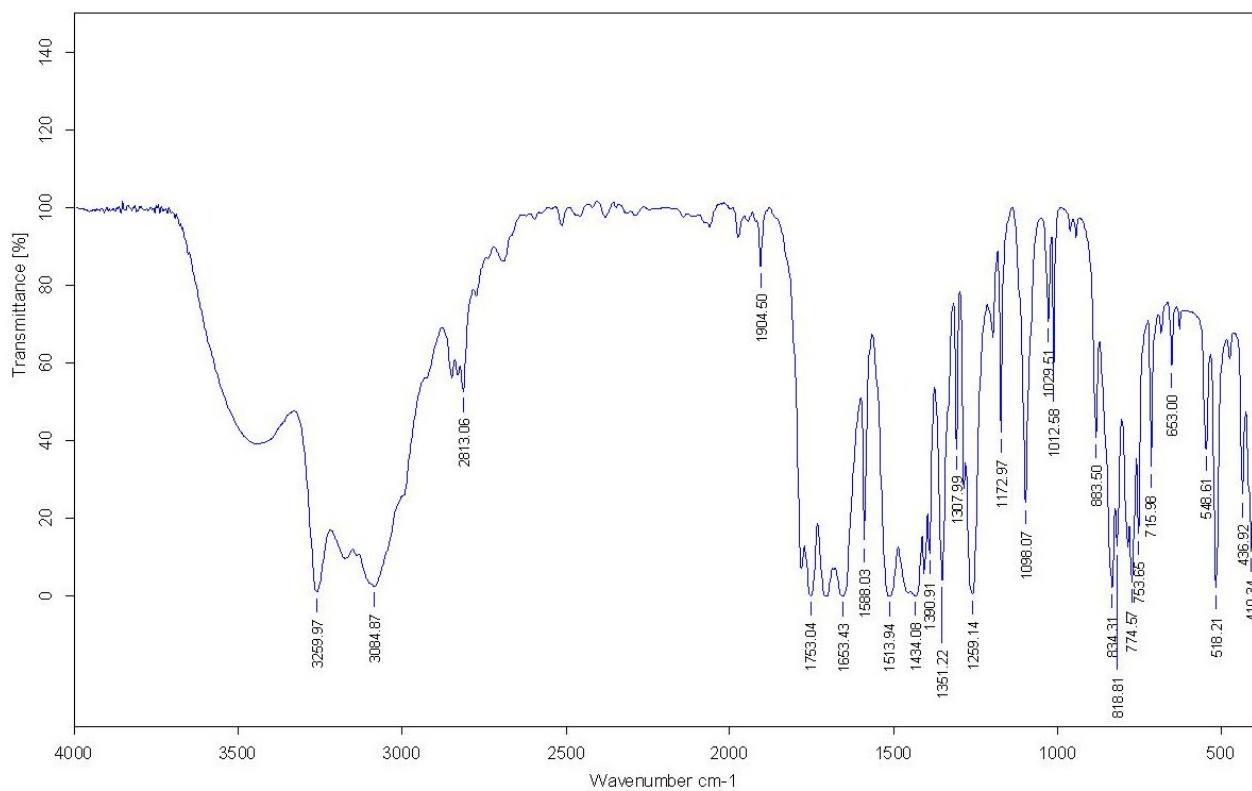


Figure 3S. IR spectra of H<sub>3</sub>L<sup>2</sup>.

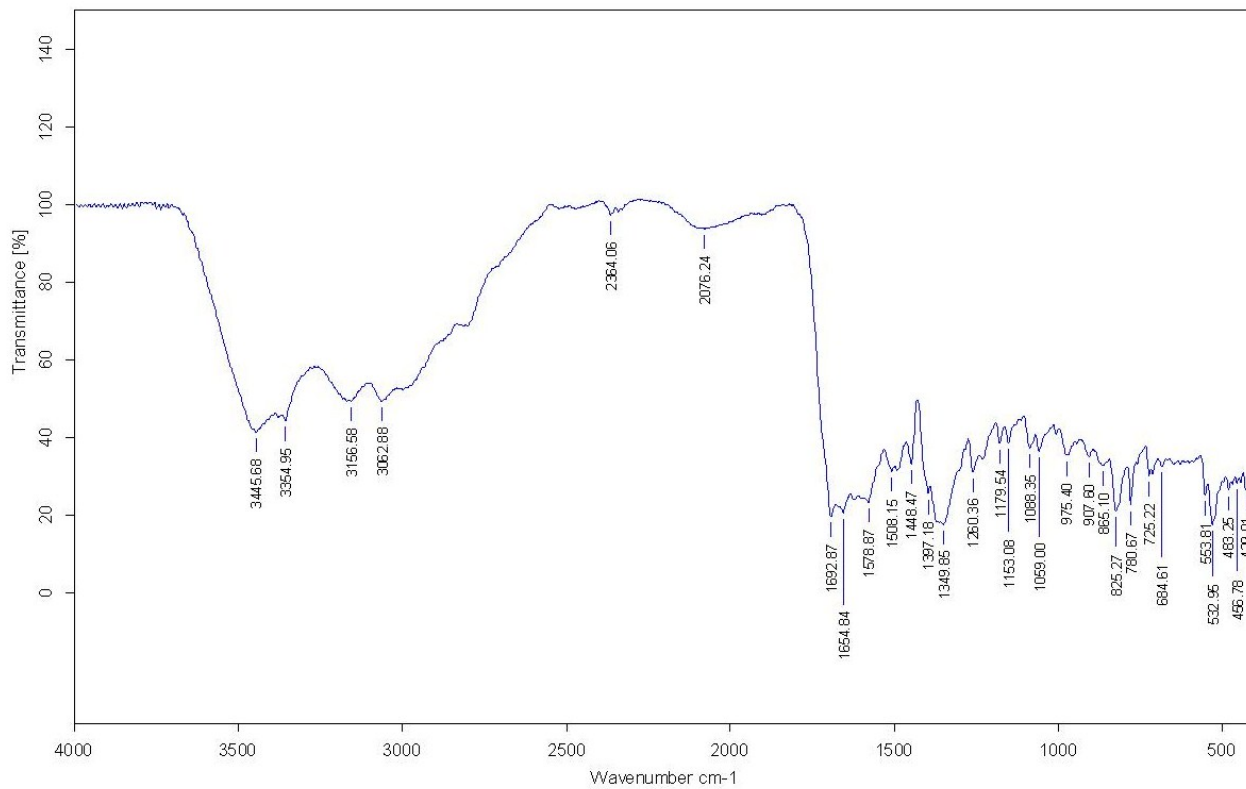


Figure 4S. IR spectra of 2.

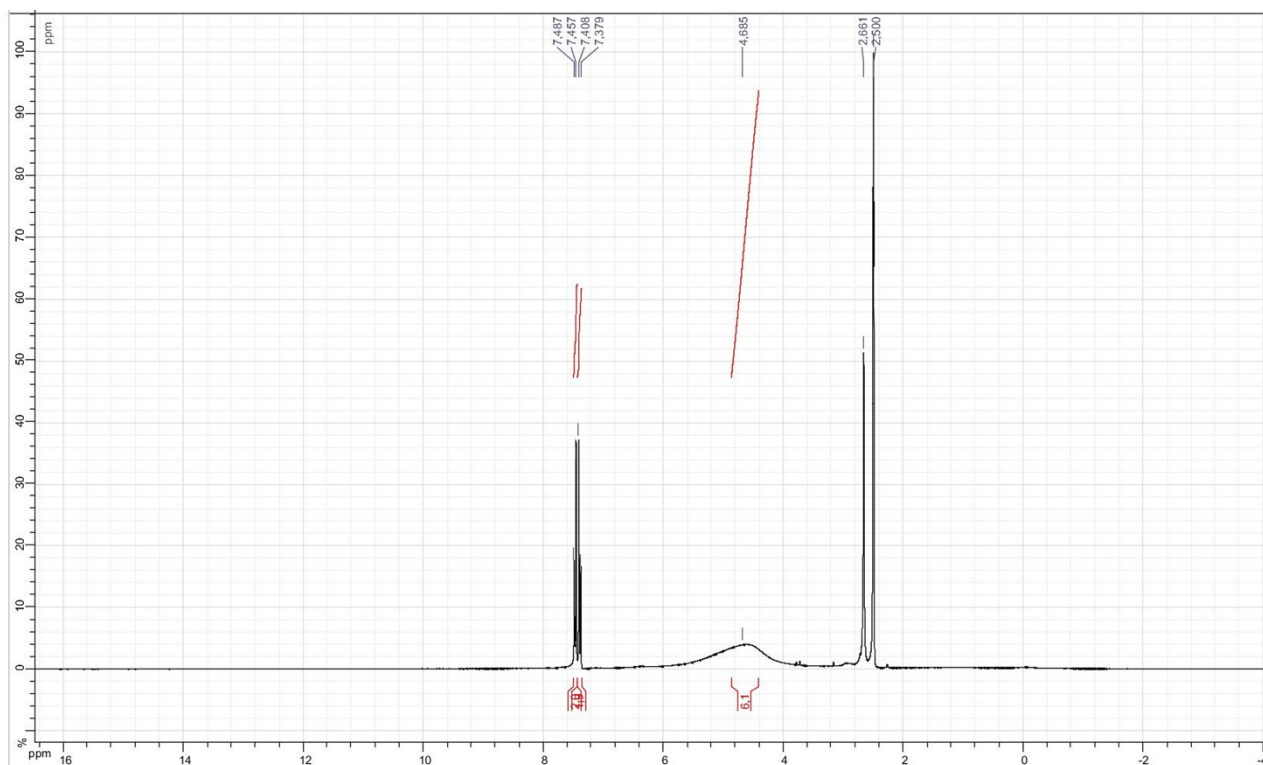


Figure 5S. <sup>1</sup>H NMR spectra of 2.



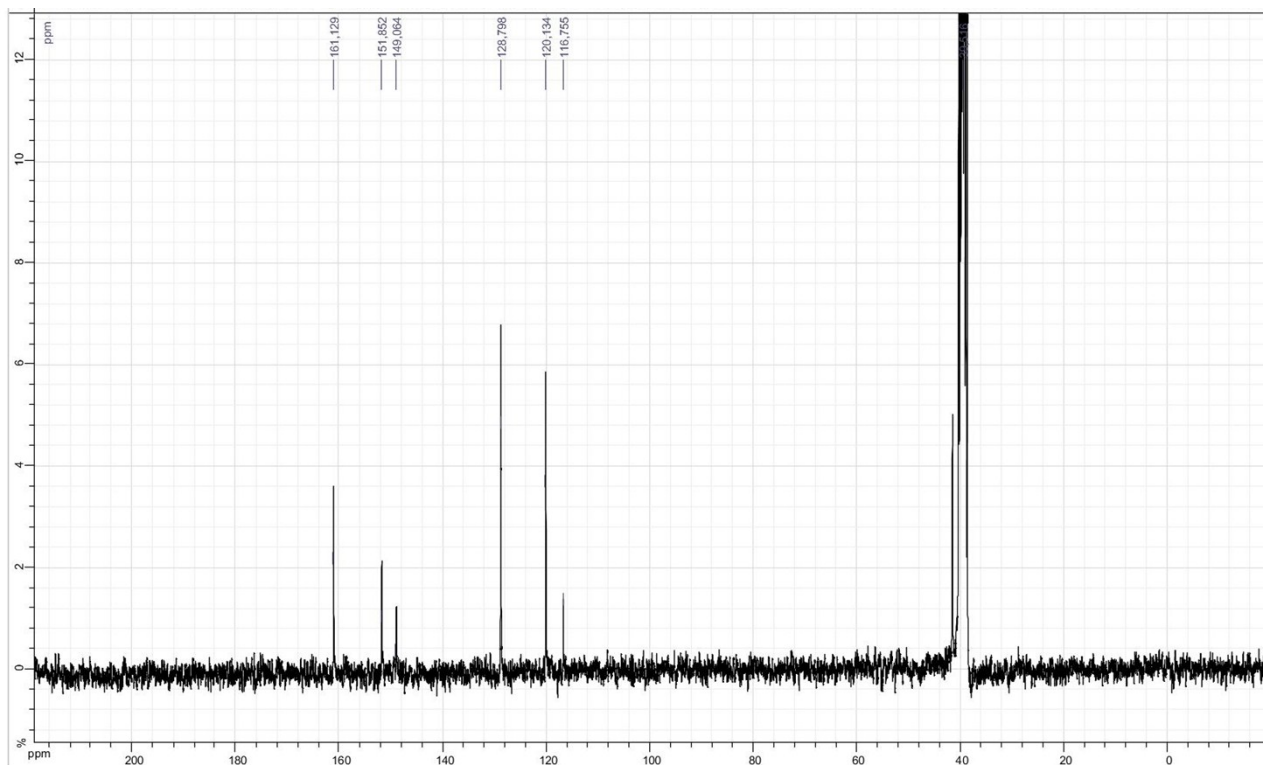


Figure 6S.  $^{13}\text{C}$  NMR spectra of **2**.

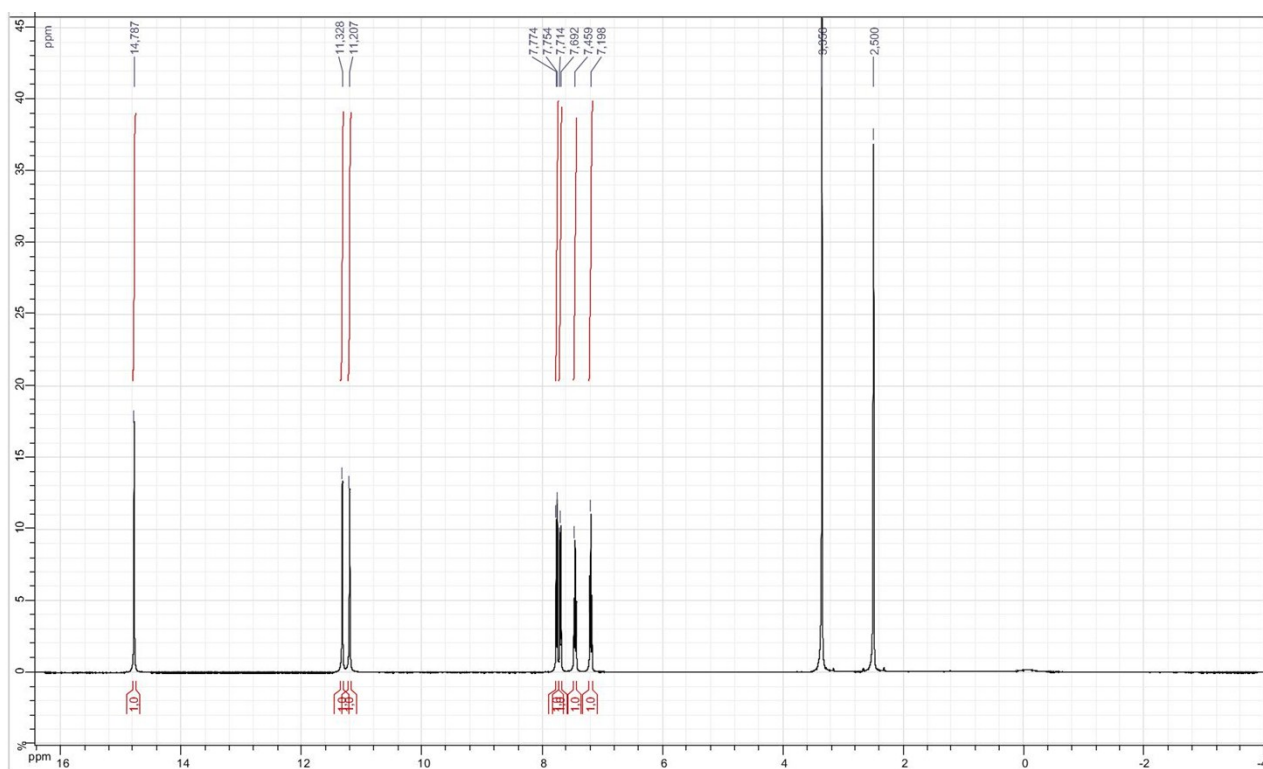


Figure 7S.  $^1\text{H}$  NMR spectra of **7**.

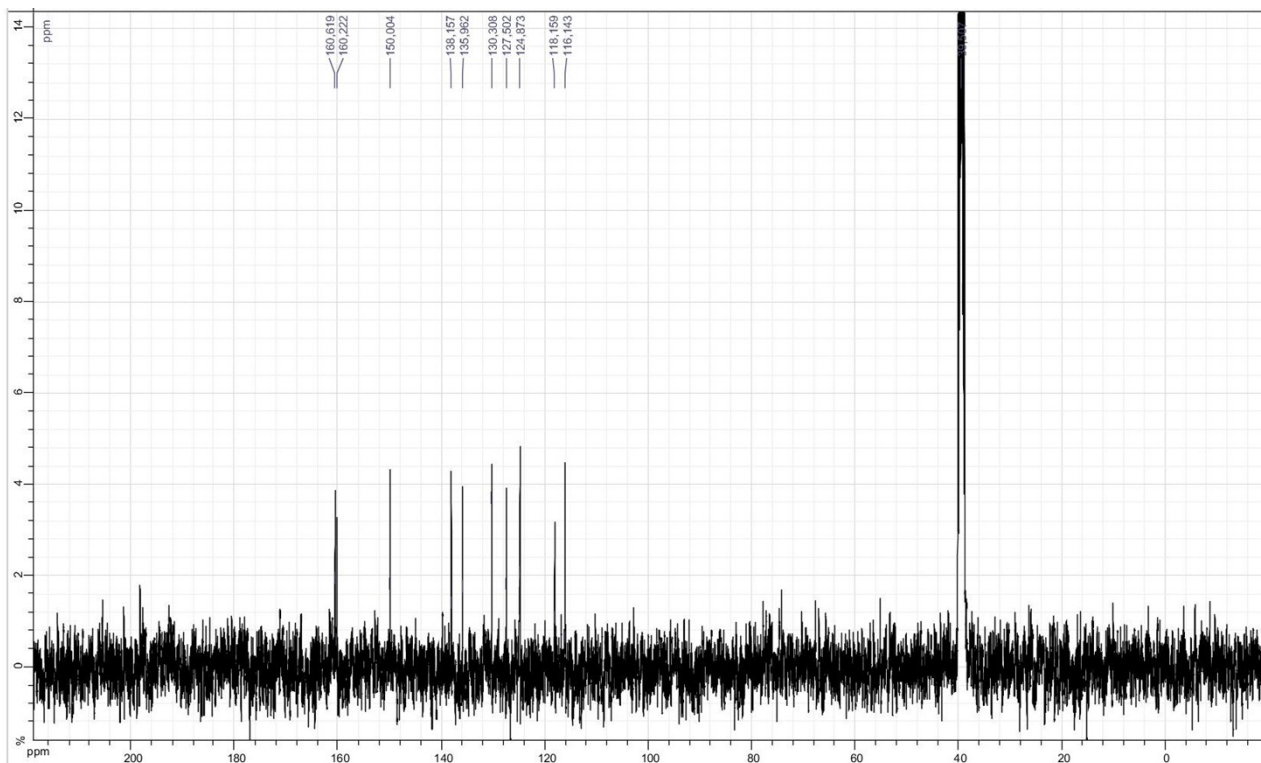


Figure 8S.  $^{13}\text{C}$  NMR spectra of 7.

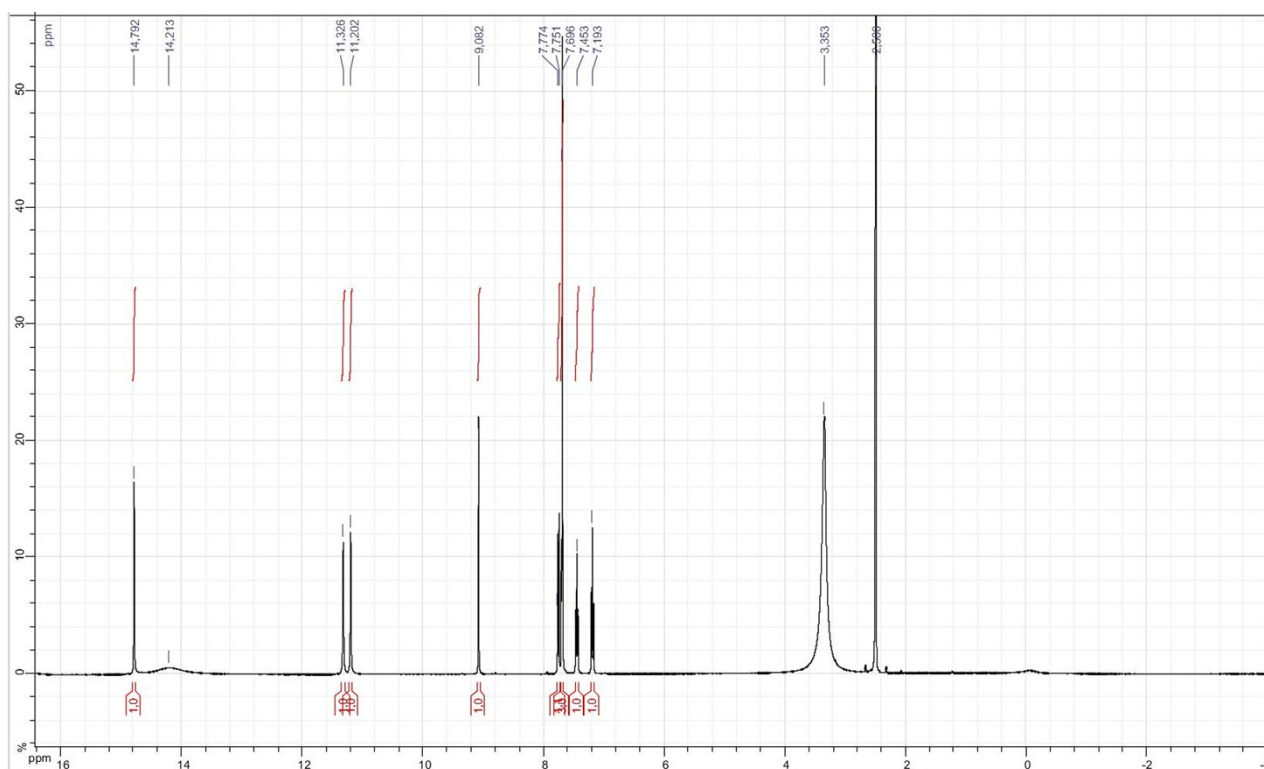


Figure 9S.  $^1\text{H}$  NMR spectra of 8.

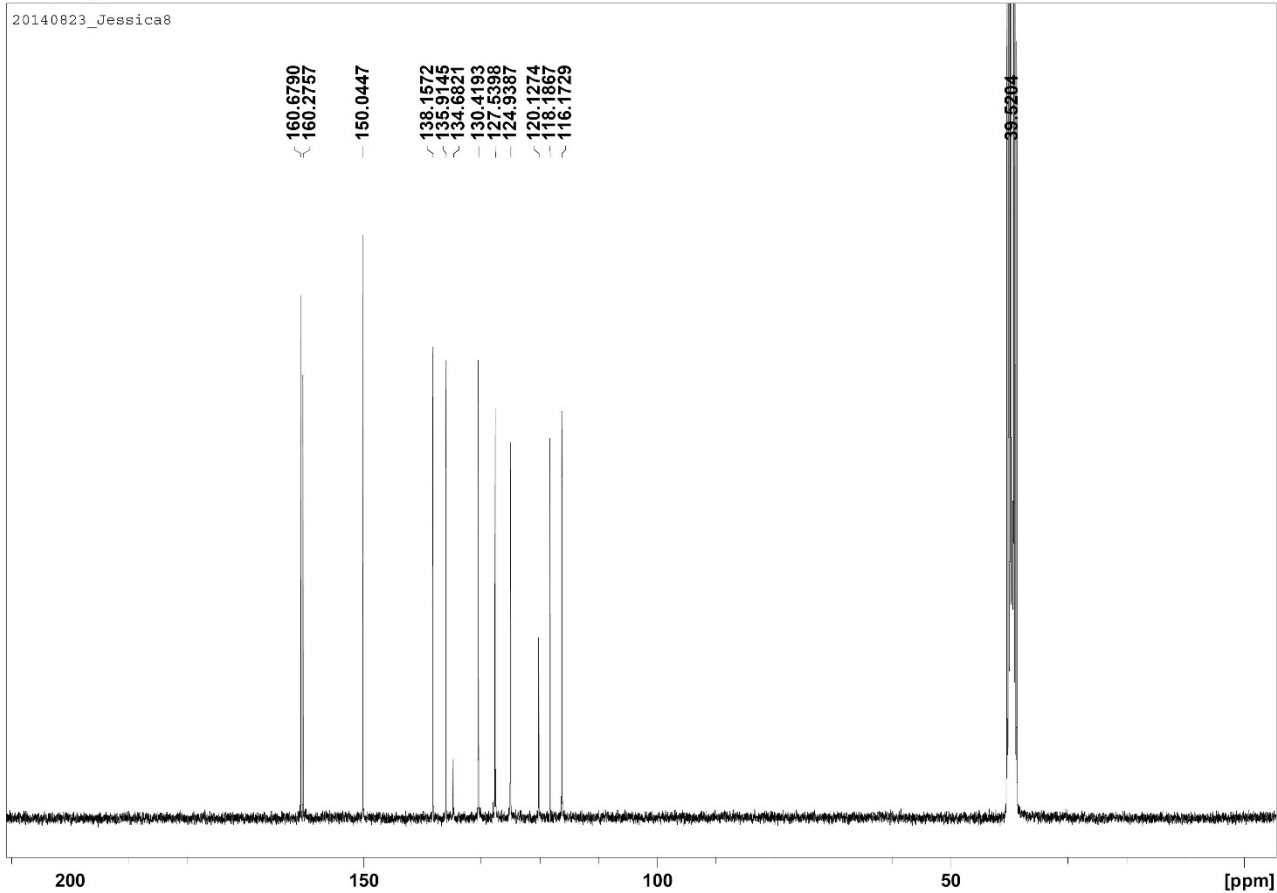


Figure 10S. <sup>13</sup>C NMR spectra of **8**.

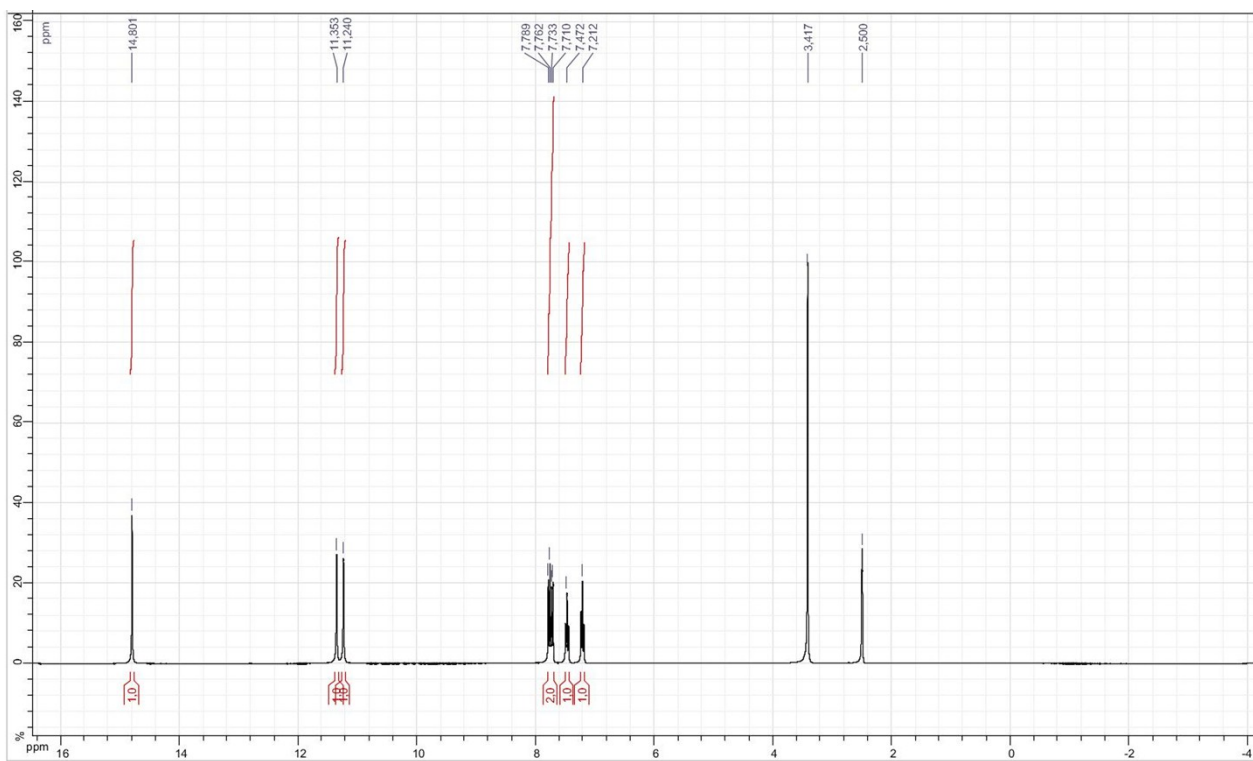
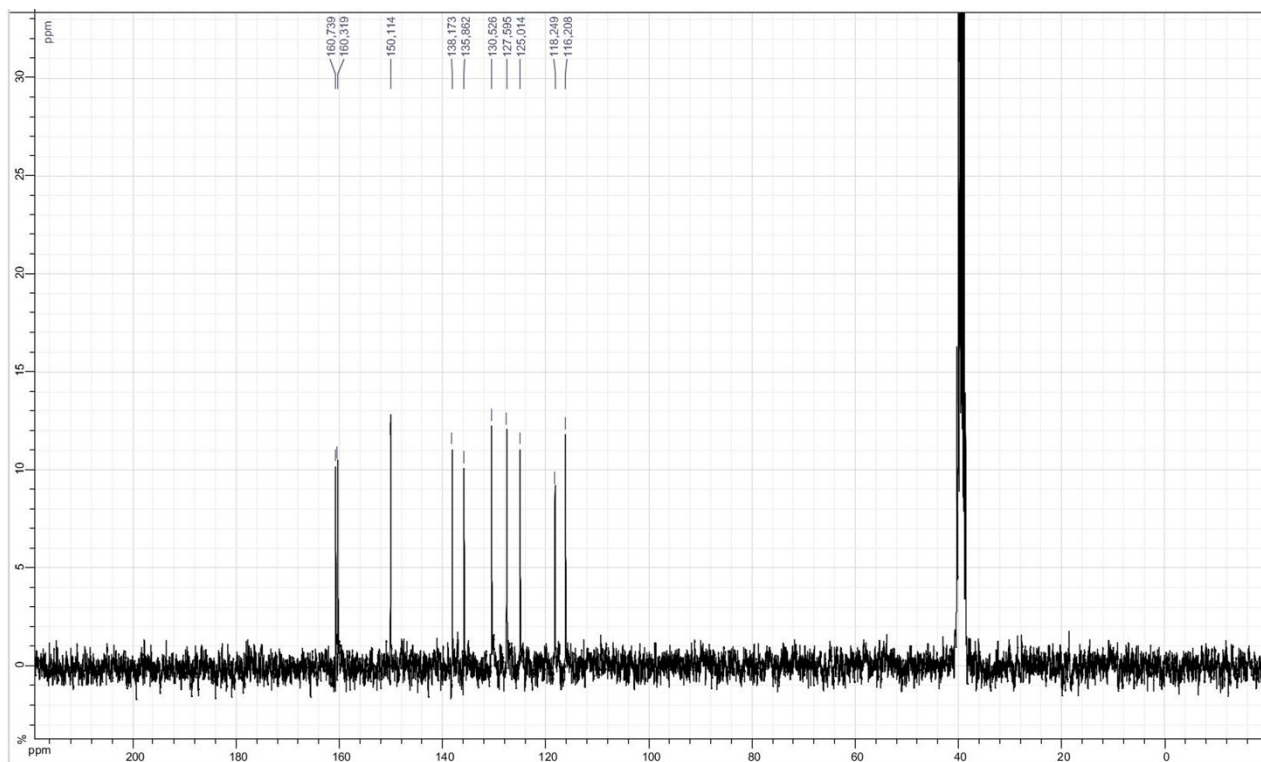
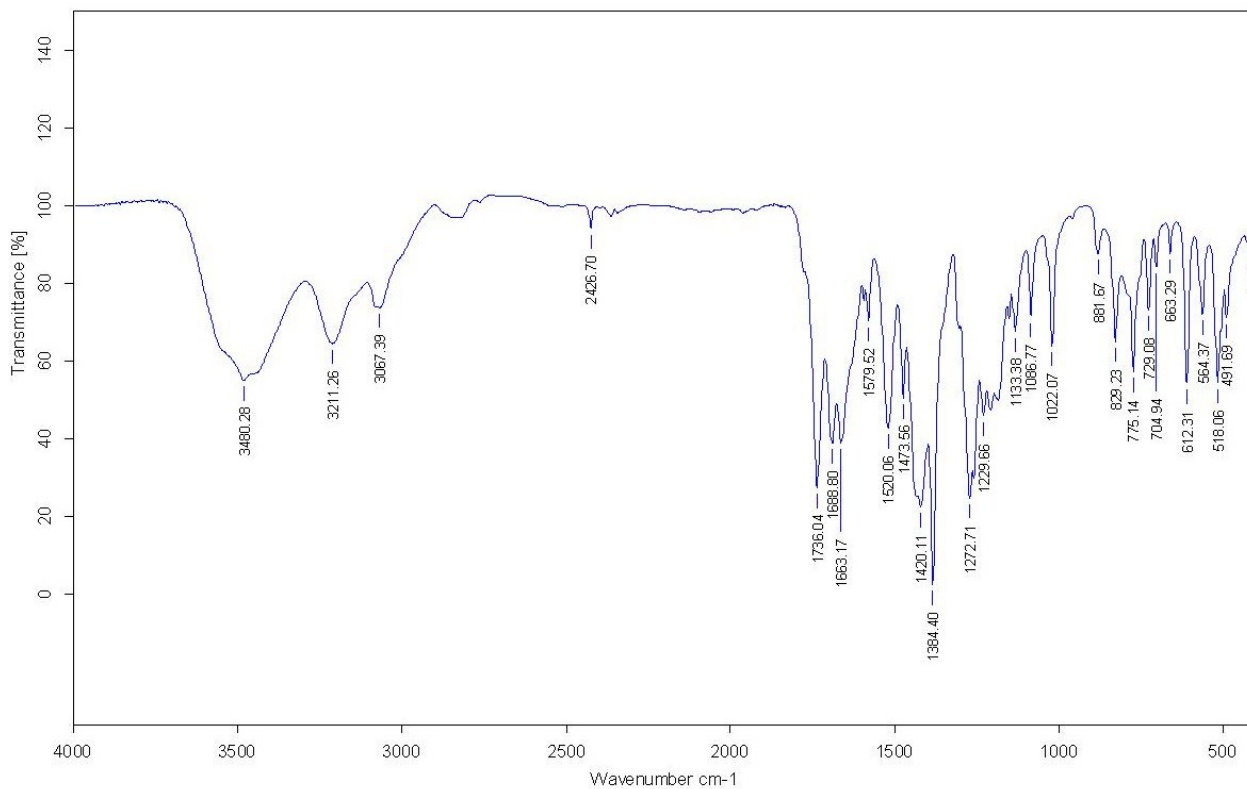


Figure 11S. <sup>1</sup>H NMR spectra of **1**.



**Figure 12S.**  $^{13}\text{C}$  NMR spectra of **1**.



**Figure 13S.** IR spectra of **7**.

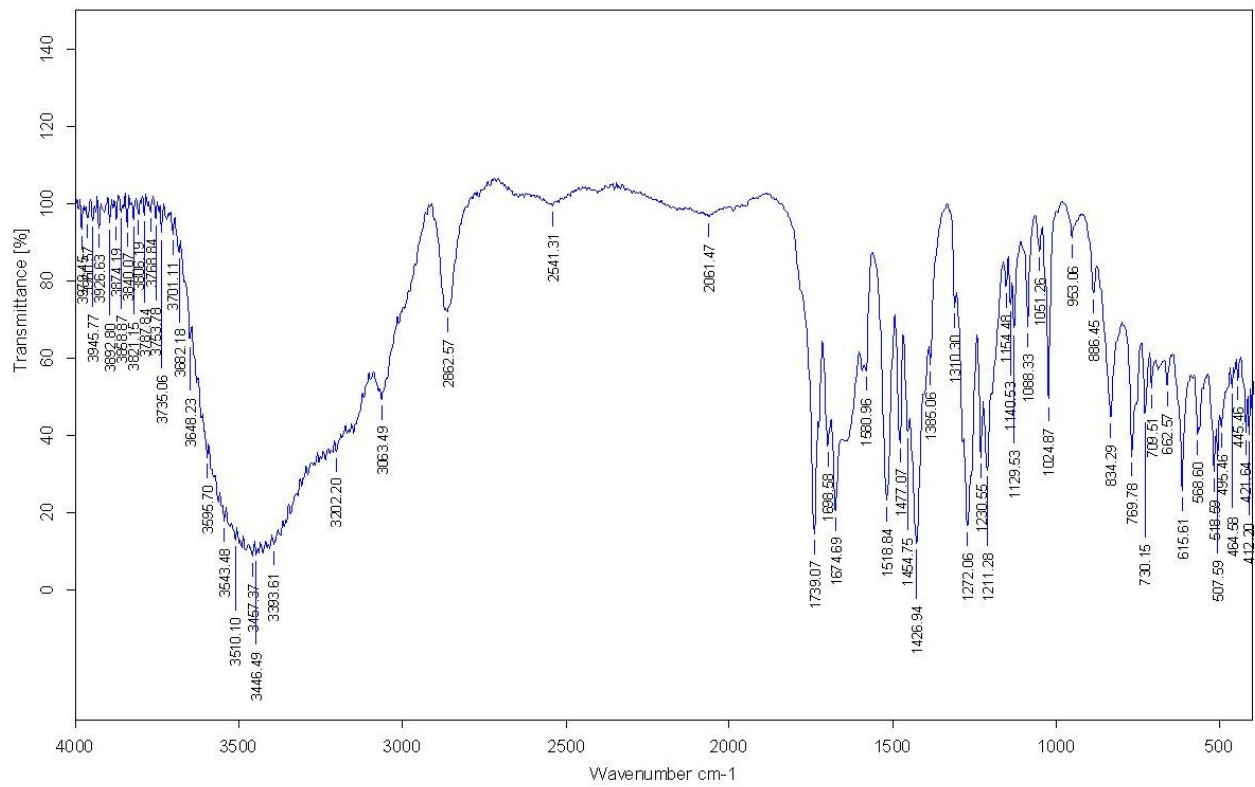


Figure 14S. IR spectra of 8.

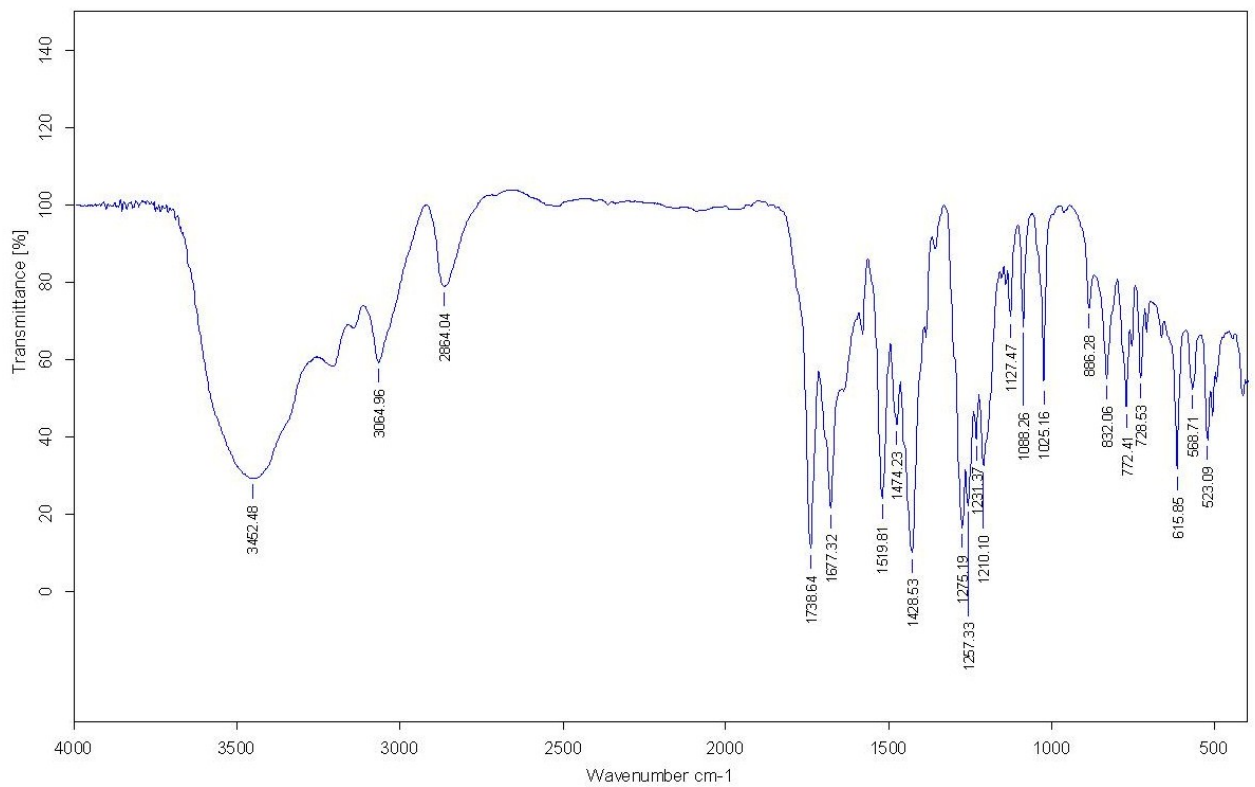


Figure 15S. IR spectra of 1.

### 3. X-ray analysis

**Table 1S.** Crystal data, experimental parameters and selected details of the refinement calculations of compounds **2**, **7** and **8**.

Compound	<b>2</b>	<b>7</b>	<b>8</b>
Empirical formula	C <sub>36</sub> H <sub>49</sub> Cl <sub>3</sub> N <sub>18</sub> O <sub>11</sub>	C <sub>10</sub> H <sub>9</sub> AgN <sub>4</sub> O <sub>7</sub> S	C <sub>13</sub> H <sub>16</sub> N <sub>6</sub> O <sub>8</sub> S
Formula weight	1016.28	437.14	416.38
Crystal system	Monoclinic	Triclinic	Triclinic
Space group	<i>P</i> 21/ <i>c</i>	<i>P</i> -1	<i>P</i> -1
<i>a</i> (Å)	10.4057(3)	8.4530(2)	7.1448(18)
<i>b</i> (Å)	21.2989(6)	9.1802(3)	11.280(4)
<i>c</i> (Å)	21.0249(6)	9.5557(3)	12.049(4)
$\alpha$ (deg)	90	69.666(3)	116.777(12)
$\beta$ (deg)	100.811(1)	69.858(2)	98.803(11)
$\gamma$ (deg)	90	79.279(2)	97.186(11)
<i>Z</i>	4	2	2
<i>V</i> (Å <sup>3</sup> )	4577.0(2)	650.93(4)	835.8(4)
<i>T</i> (K)	296	150	150
$\rho_{\text{calc}}$ (g/cm <sup>3</sup> )	1.475	2.230	1.655
$\mu$ (Mo K $\alpha$ ) (mm <sup>-1</sup> )	0.279	1.757	0.256
Rfl collected/unique/obs	66617/5164/3794	11649/4749/4228	13696/3413/2364
<i>R</i> 1 <sup>a</sup> ( <i>I</i> $\geq$ 2 $\sigma$ )	0.0857	0.0465	0.0590
wR2 <sup>b</sup> ( <i>I</i> $\geq$ 2 $\sigma$ )	0.2558	0.1401	0.1523
GOF on <i>F</i> <sup>2</sup>	1.135	1.093	0.957

<sup>[a]</sup>  $R1 = \sum ||F_o| - |F_c|| / \sum |F_o|$ . <sup>[b]</sup>  $wR2 = [\sum [w(F_o^2 - F_c^2)^2] / \sum [w(F_o^2)^2]]^{1/2}$ .

**Table 2S.** Selected distances (Å) and angles (°) for compounds **2**, **7** and **8**.

	<b>2</b>	<b>7</b>	<b>8</b>		
C8–O1	1.232(7)	C7–N2	1.327(4)	C7–O1	1.232(4)
C9–O2	1.238(7)	C8–O1	1.239(3)	C9–O2	1.217(4)
C7–N2	1.395(8)	C9–O2	1.224(3)	C8–N2	1.326(4)
N1–N2	1.202(8)	O1–Ag1	2.589(3)	C10–O3	1.231(4)
C4–N1	1.498(9)	O3–Ag1	2.566(2)	N1–N2	1.308(4)
C10–O3	1.229(7)	O10–Ag1	2.318(3)	N1–N2–C8	120.5(3)
N2–N1–C4	111.5(7)	O11–Ag1	2.343(2)	N2–C8–C7	124.2(3)
N1–N2–C7	118.1(7)	O13–Ag1	2.359(2)	O1–C7–C8	123.8(3)

**Table 3S.** Hydrogen bond interactions (Å, °) in complexes **2**, **7** and **8**.

D-H...A	<i>d</i> (H...A)	<i>d</i> (D...A)	∠(D-H...A)	Symmetry operation
<b>2</b>				
O1W...H1A...O9	1.90(4)	2.758(7)	156(6)	<i>x, 1/2-y, 1/2+z</i>
O2W...H2A...O6	1.91(7)	2.801(6)	167(7)	<i>x, 1/2-y, -1/2+z</i>
O2W...H2B...O1	2.12(8)	2.821(6)	134(8)	<i>intra</i>
O2W...H2B...N1	2.21(6)	2.972(10)	143(9)	<i>intra</i>
N3...H3N...O5	1.90(11)	2.900(6)	165(8)	<i>x, 1/2-y, -1/2+z</i>
N4...H4N...O6	2.08(4)	2.954(6)	170(11)	<i>x, 1/2-y, -1/2+z</i>
N7...H7N...O3	1.98(3)	2.872(6)	177(15)	<i>1+x, 1/2-y, 1/2+z</i>
N8...H8N...O1	1.84(11)	2.814(6)	174(10)	<i>x, 1/2-y, 1/2+z</i>
N11...H11N...O7	1.96(12)	2.824(6)	166(8)	<i>1-x, 1-y, 1-z</i>
N12...H12N...O9	2.08(12)	2.938(6)	164(9)	<i>-x, 1-y, 1-z</i>
N31...H31C...O2	2.08(7)	2.868(7)	148(9)	<i>intra</i>
N31...H31D...O1W	2.19(11)	3.042(9)	148(10)	<i>intra</i>
N32...H32C...O2	2.52(11)	3.118(7)	122(8)	<i>intra</i>
N32...H32C...N2	2.38(11)	3.296(8)	164(9)	<i>intra</i>
N32...H32D...O5	2.28(10)	3.011(7)	133(8)	<i>intra</i>
N32...H32D...N6	2.31(11)	3.193(7)	154(9)	<i>intra</i>
N32...H32E...N35	1.88(11)	2.836(8)	172(5)	<i>-1+x,y,z</i>
N33...H33C...O5	2.34	3.175(8)	156	<i>intra</i>
N33...H33D...O8	2.37	3.094(7)	138	<i>intra</i>
N34...H34C...N31	1.84(11)	2.811(9)	168(10)	<i>-x, 1/2+y, 3/2-z</i>
N34...H34D...O2W	1.90(8)	2.785(8)	170(8)	<i>1-x, 1/2+y, 3/2-z</i>
N34...H34E...O8	2.38(11)	2.940(7)	125(9)	<i>intra</i>
N34...H34E...N9	2.28(11)	3.074(8)	159(9)	<i>intra</i>
N35...H35C...O4	2.42(12)	2.992(7)	124(10)	<i>intra</i>
N36...H36C...O1W	2.40(11)	2.991(9)	122(7)	<i>1-x, 1/2+y, 3/2-z</i>
N36...H36D...O7	1.93(8)	2.810(7)	170(8)	<i>intra</i>
N36...H36E...O4	2.13(10)	2.770(7)	124(8)	<i>intra</i>
N36...H36E...N5	2.13(12)	2.976(8)	149(10)	<i>intra</i>
<b>7</b>				
N1...H1N...O1	1.87(4)	2.613(4)	142(6)	<i>intra</i>
N1...H1N...O13	2.22(6)	2.815(4)	125(5)	<i>intra</i>
N3...H3N...O12	2.17(3)	3.037(4)	166(6)	<i>1-x, 1-y, 1-z</i>
N4...H4N...O13	2.50(6)	3.059(4)	121(5)	<i>x, 1+y, z</i>
N4...H4N...O2	2.09(6)	2.912(4)	153(5)	<i>1-x, 2-y, 2-z</i>
O10...H10A...O11	1.98(5)	2.911(5)	159(5)	<i>-x, 1-y, 1-z</i>
O10...H10B...O2	1.86(5)	2.815(4)	169(4)	<i>x, y, -1+z</i>
<b>8</b>				
O1W...H1W1...O12	2.02(4)	2.830(4)	159(4)	<i>intra</i>
N1...H1N...O1	2.01(5)	2.650(5)	124(4)	<i>intra</i>
N1...H1N...O13	1.94(4)	2.714(4)	138(4)	<i>intra</i>
O1W...H1W2...O11	2.27(4)	2.934(4)	146(5)	<i>1+x,y,z</i>
O2W...H2W1...O3	1.88(3)	2.842(3)	166(4)	<i>1-x, 1-y, -z</i>
N3...H3N...O1W	1.87(4)	2.776(4)	178(5)	<i>-1+x,y,-1+z</i>
O2W...H2W2...O11	1.83(2)	2.718(4)	175(3)	<i>1-x, 1-y, 1-z</i>
N4...H4N...O3	2.09(4)	2.911(4)	175(5)	<i>1-x, 1-y, -z</i>
N11...H11N...O2W	1.84(4)	2.706(4)	172(4)	<i>intra</i>
N12...H12N...O13	2.21(4)	2.798(4)	127(4)	<i>-1+x,y,z</i>
N12...H12N...O2	2.19(5)	2.888(5)	140(3)	<i>-x,-y,-z</i>

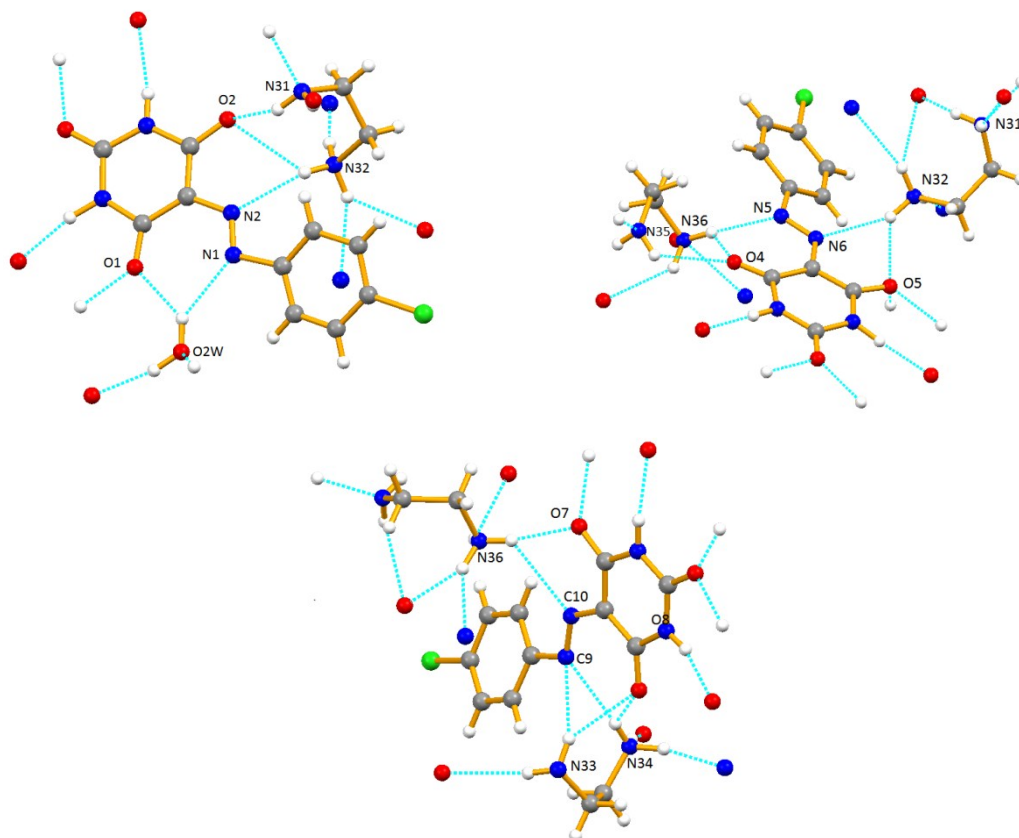


**Figure 16S.** Hydrogen bond interactions in **2** (in dashed blue lines; see also Table 3S) grouped by hydrazone anion and monoprotonated ethylenediamine cation.



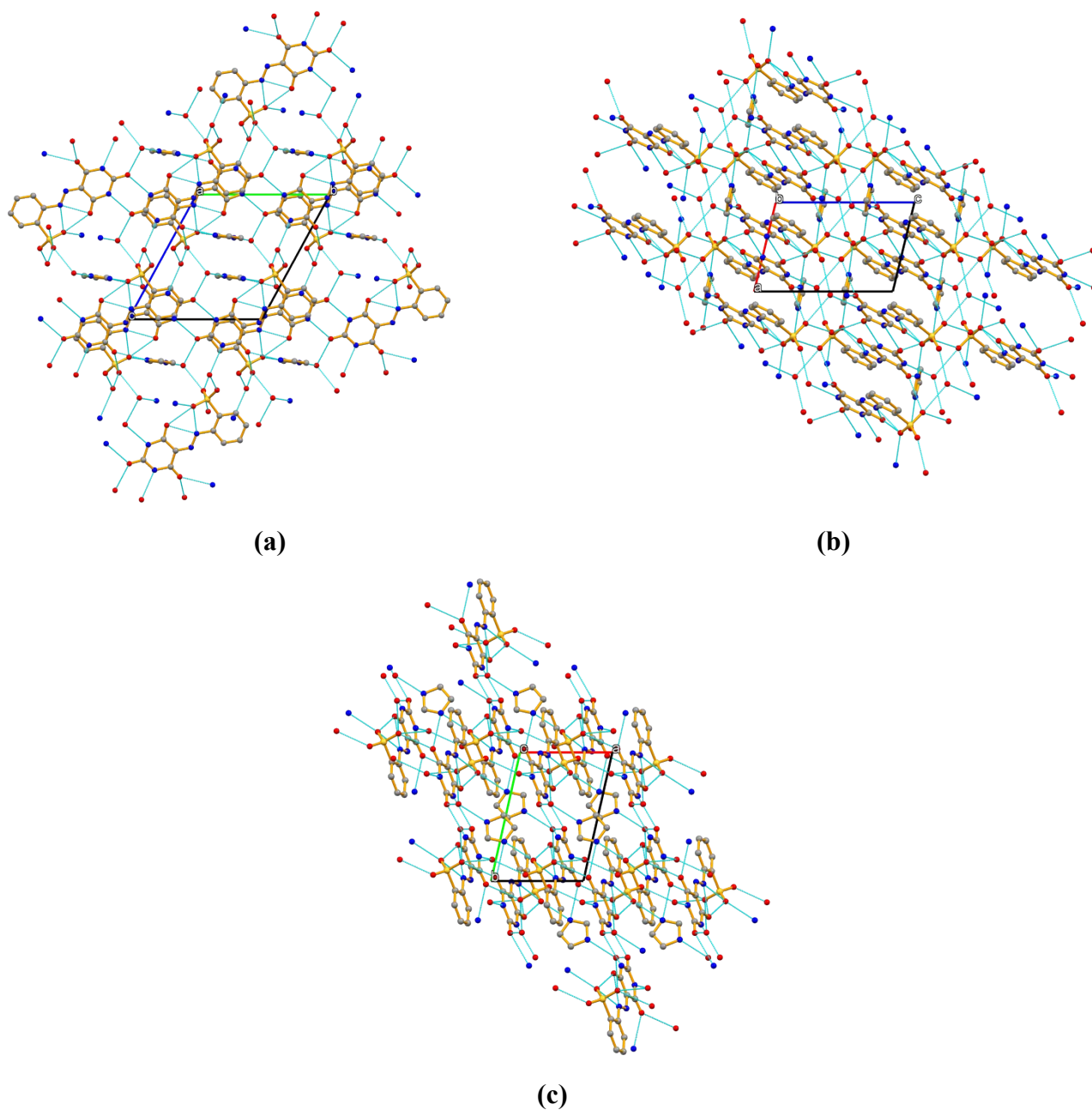


**Figure 17S.** 3D network arrangement in **2** viewed down the crystallographic  $a$ ,  $b$  and  $c$  axis, respectively. Hydrogen atoms were omitted for clarity.

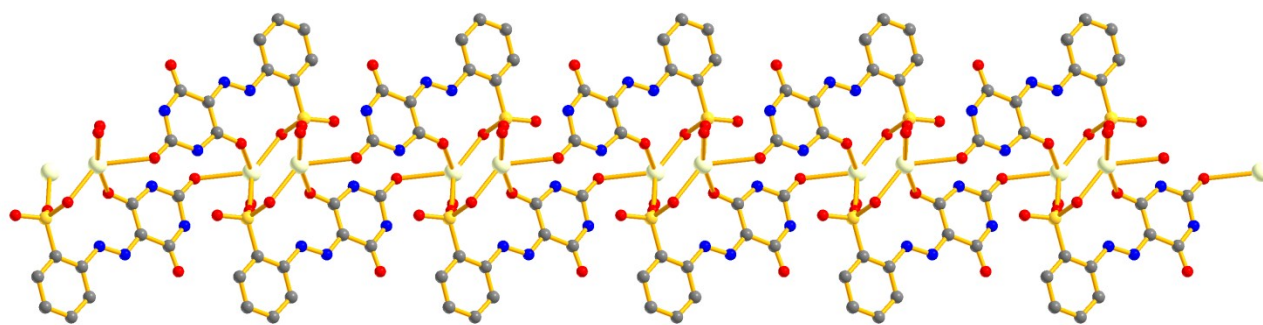


**Figure 18S.** 1D polymeric chain arrangement in **7**. Hydrogen atoms were omitted for clarity.

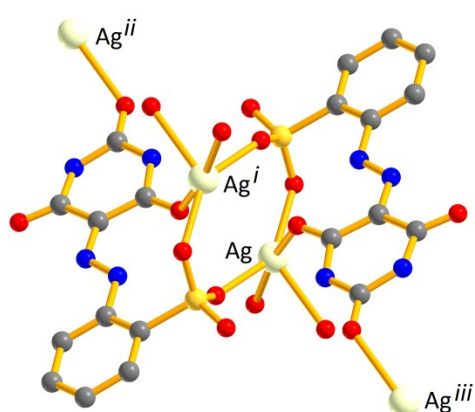


**Figure 19S.** The bridging mode of the sulfonyl groups in **7** which generate  $\{Ag_2S_2O_4\}$  dimetallic cores. i)  $1-x, 1-y, 1-z$ ; ii)  $x, -1+y, z$ ; iii)  $1-x, 2-y, 1-z$

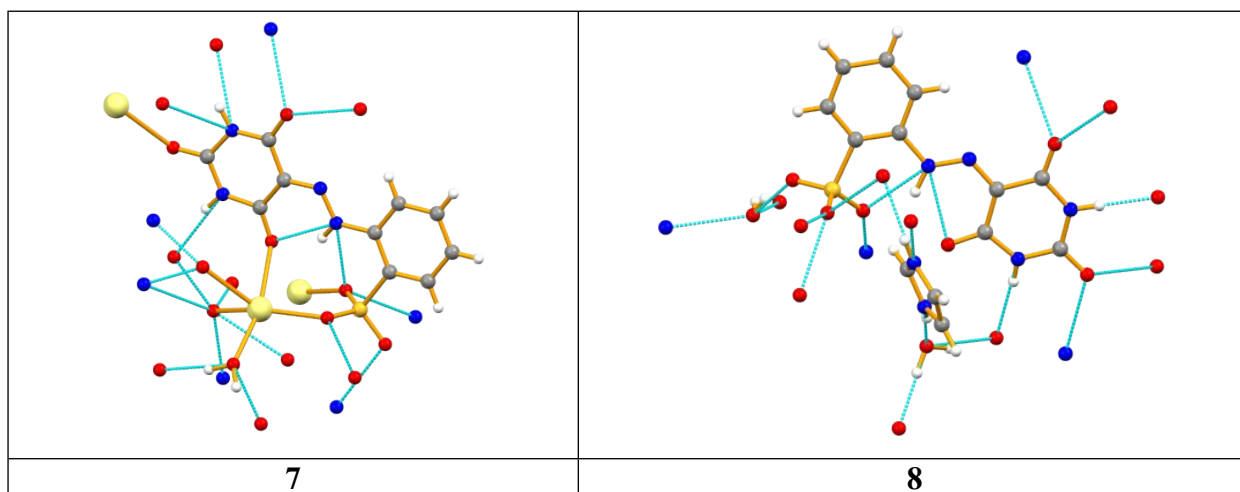
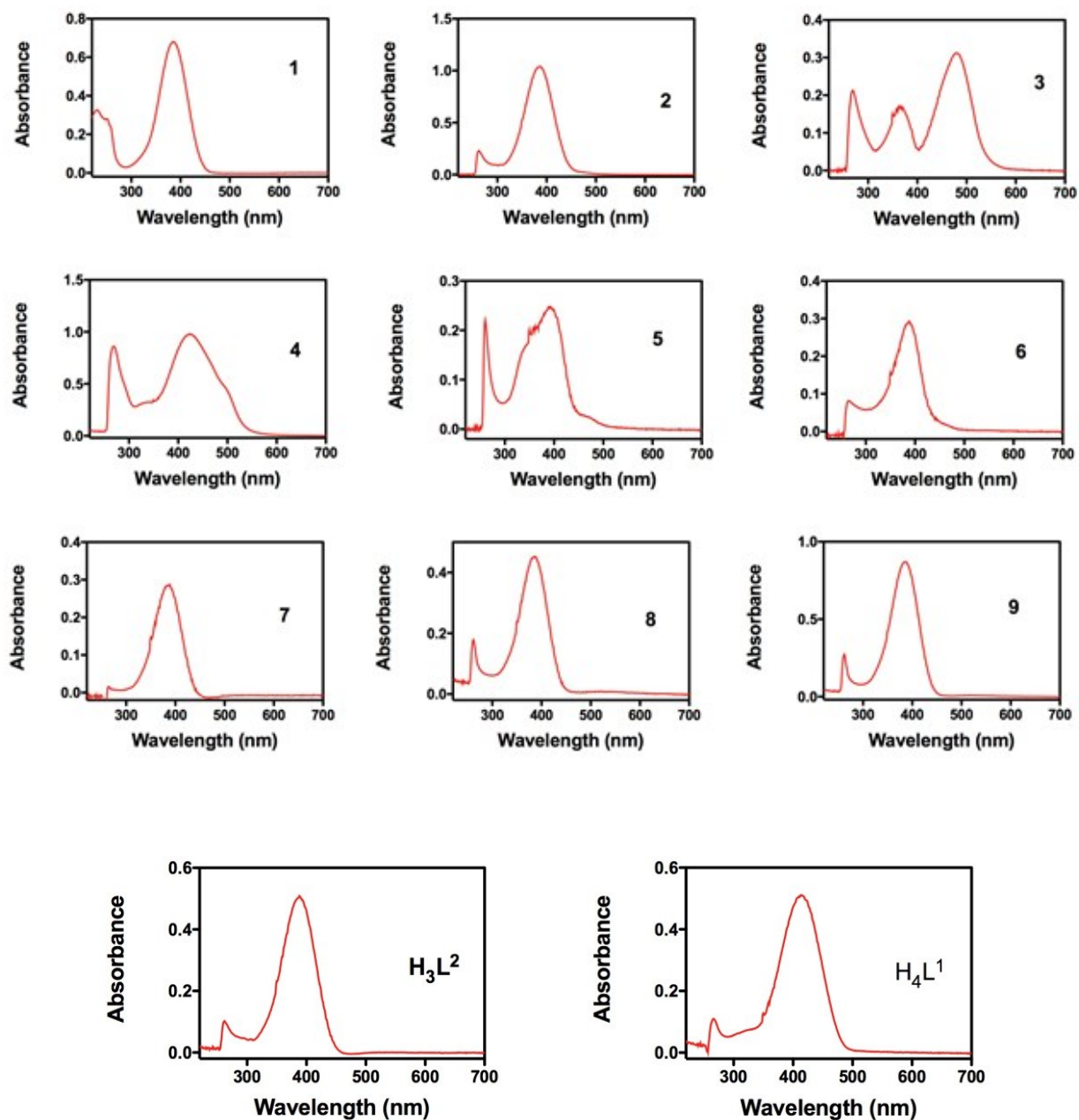


**Figure 20S.** Hydrogen bond interactions (in dashed blue lines; see also Table 3S) in **7** and **8**.

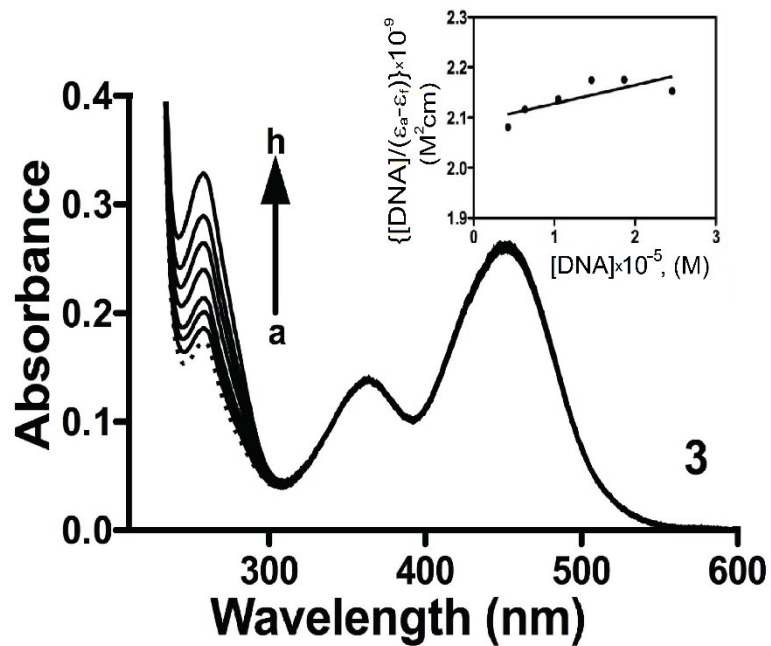
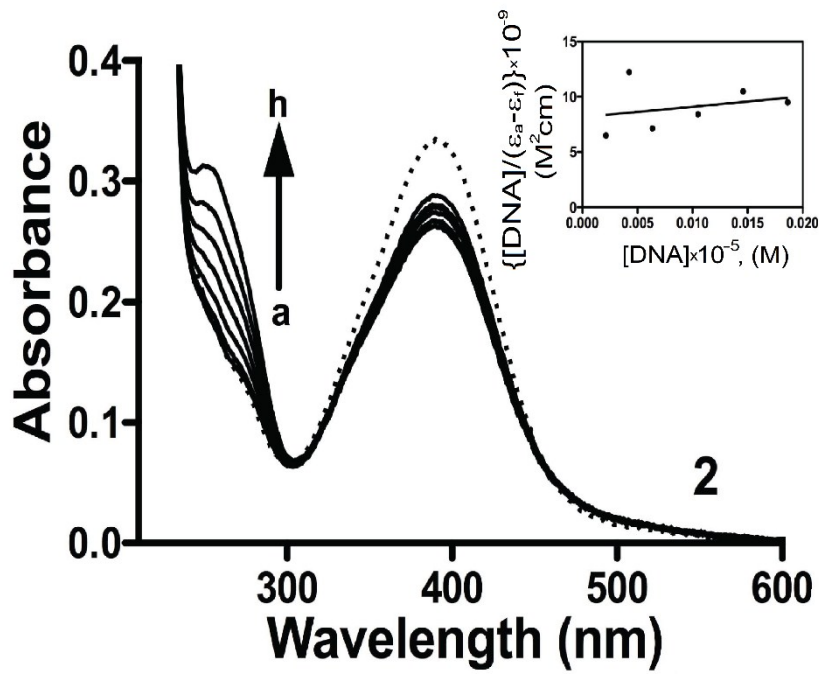
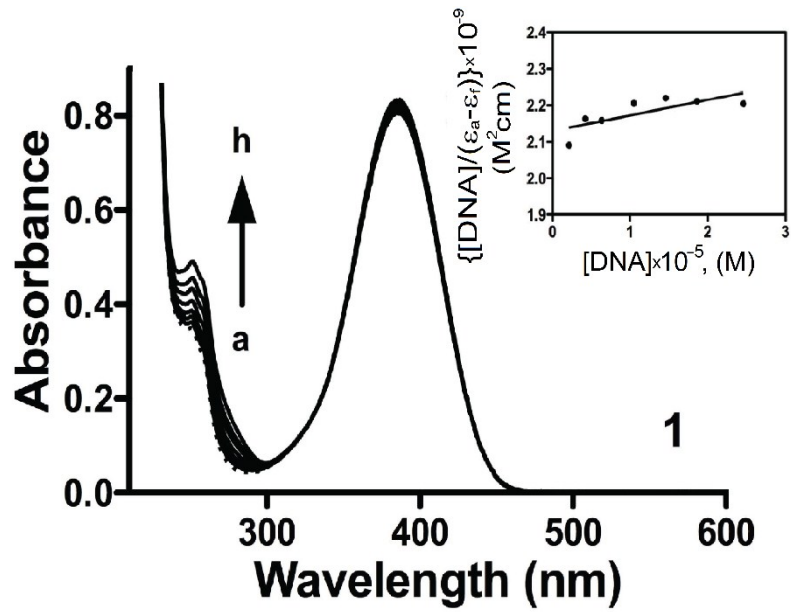
## 4. Electronic absorption spectra

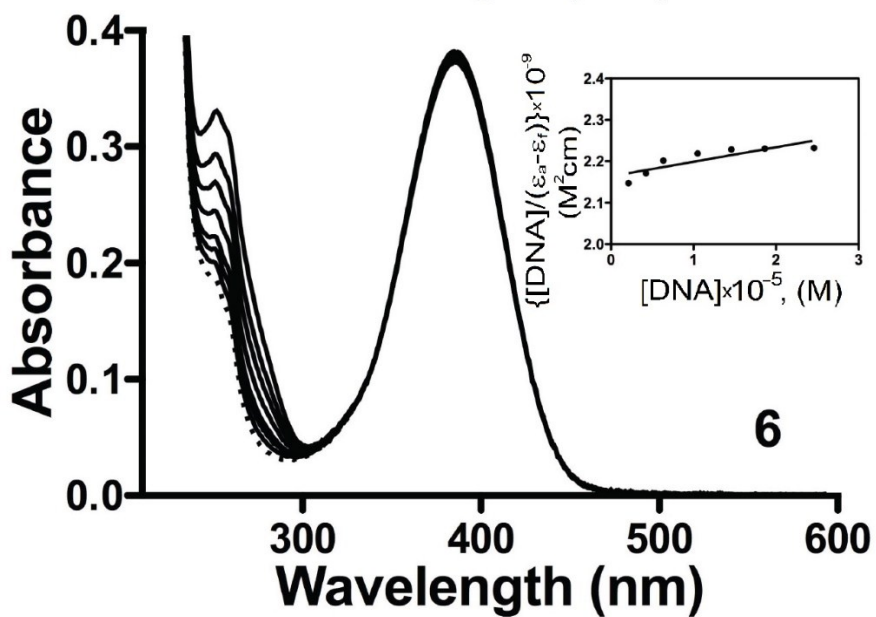
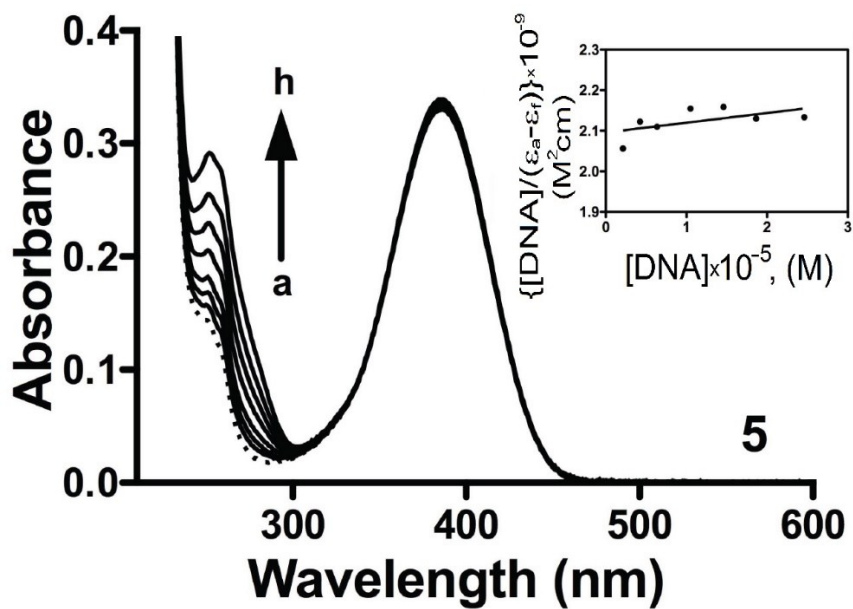
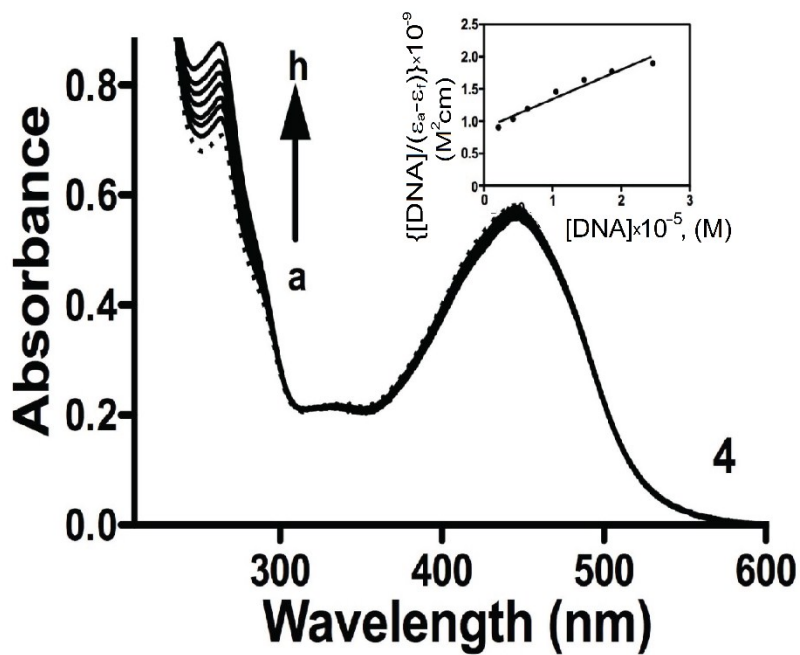
**Table 4S.** Electronic absorption spectral data of proligands  $\text{H}_4\text{L}^1$  and  $\text{H}_3\text{L}^2$  and complexes 1–9.

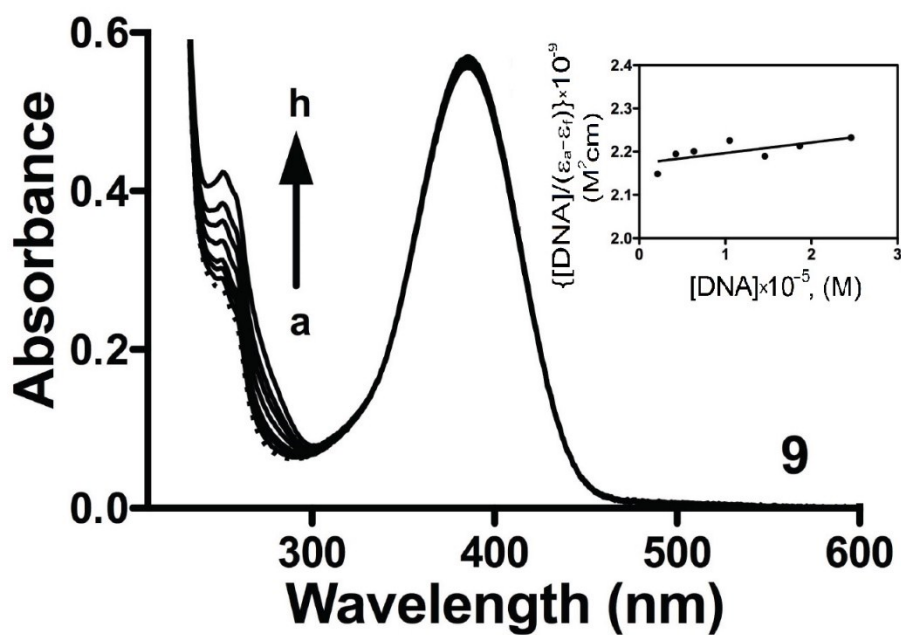
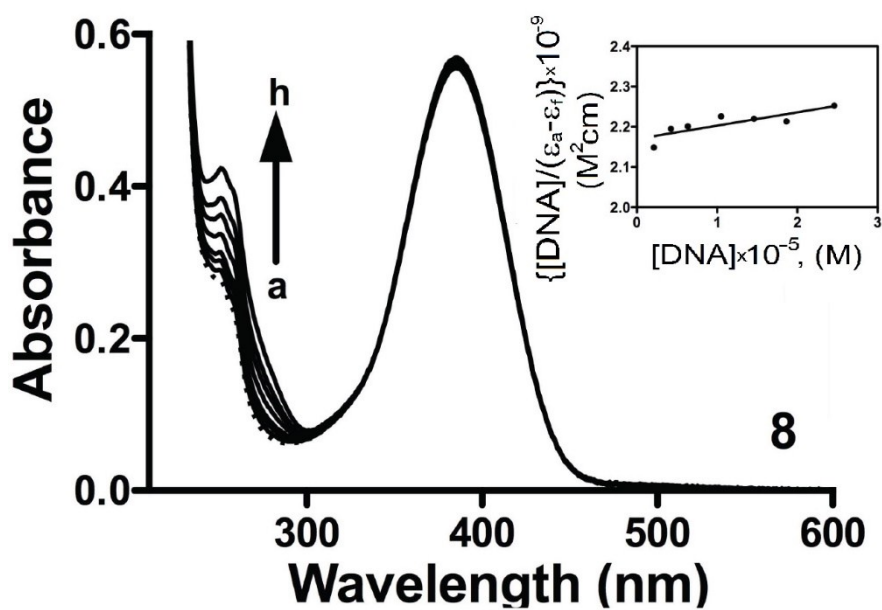
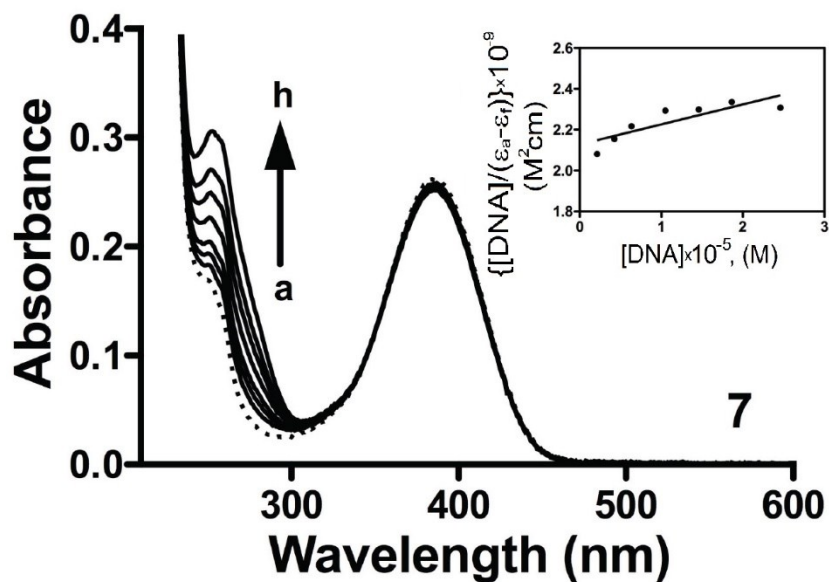
Compound	$\lambda_{\text{max}}$ (nm)	$\epsilon$ ( $\text{M}^{-1} \text{cm}^{-1}$ ) $\times 10^{-3}$
$\text{H}_4\text{L}^1$	414	37.6
	266	8.10
$\text{H}_3\text{L}^2$	388	37.5
	262	7.51
1	389	50.1
	234	2.41
2	388	76.5
	262	16.9
3	480	23.0
	366	12.5
	269	15.7
4	424	72.2
	350	25.3
	269	63.4
5	393	18.3
	350	14.9
	260	16.3
6	388	21.6
	265	6.04
7	388	21.1
8	388	33.3
	262	13.2
9	384	64.1
	262	20.2



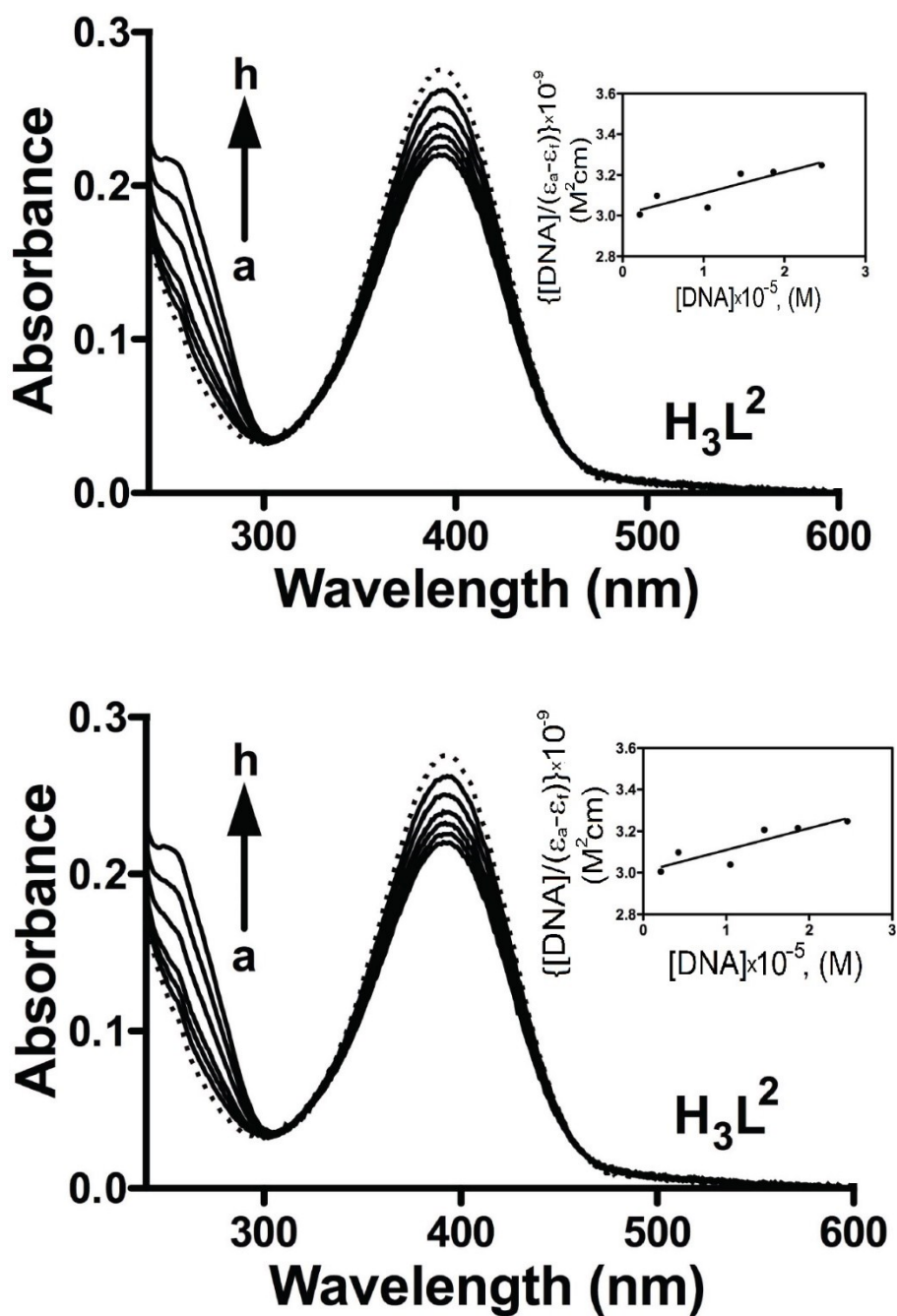
**Figure 21S.** UV-vis spectra for different compounds 15  $\mu$ M in DMSO ( $H_4L^1$ ,  $H_3L^2$ , 2-9) and water (1) solution.





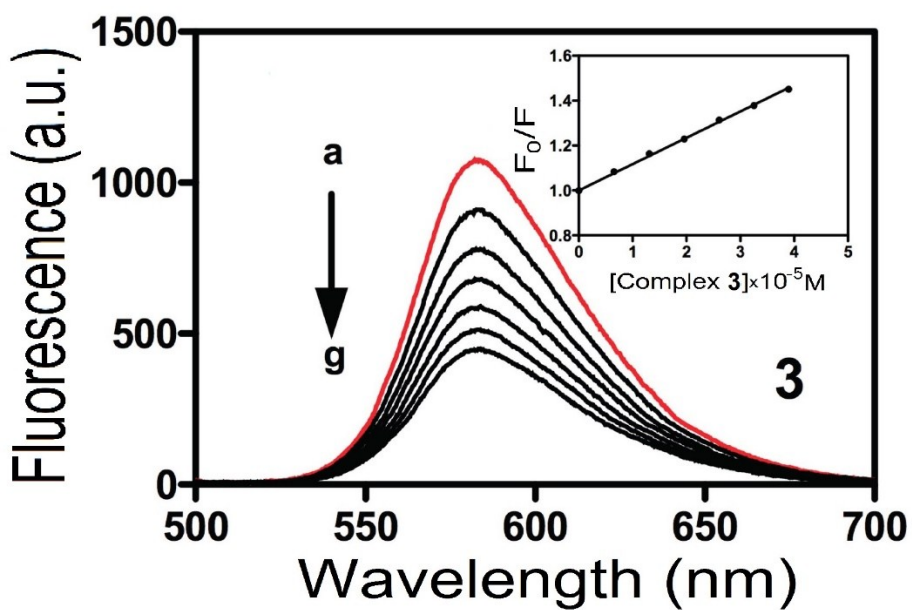
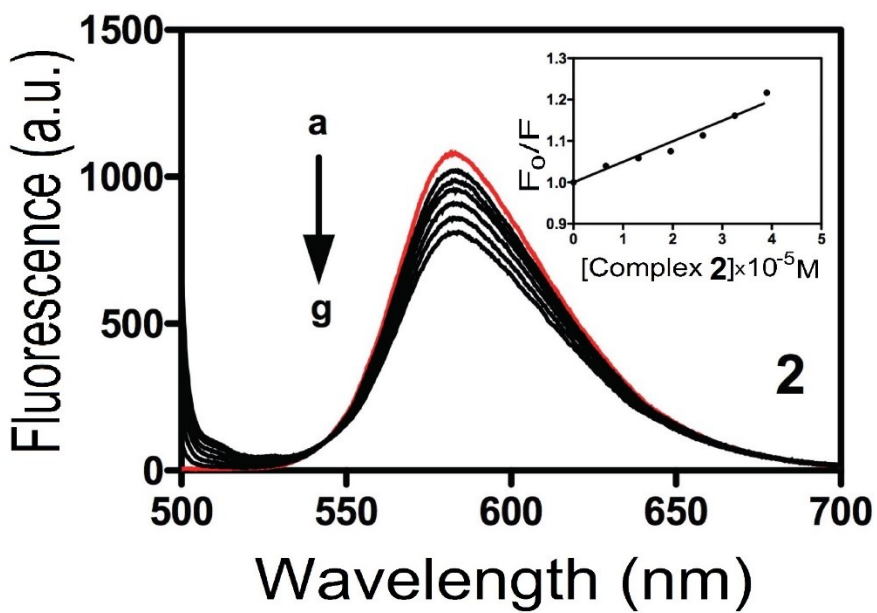
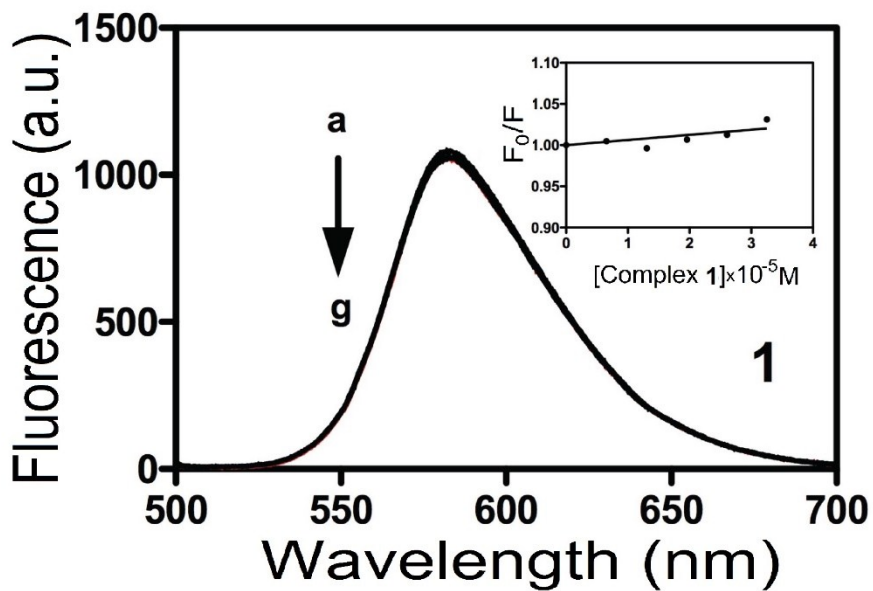


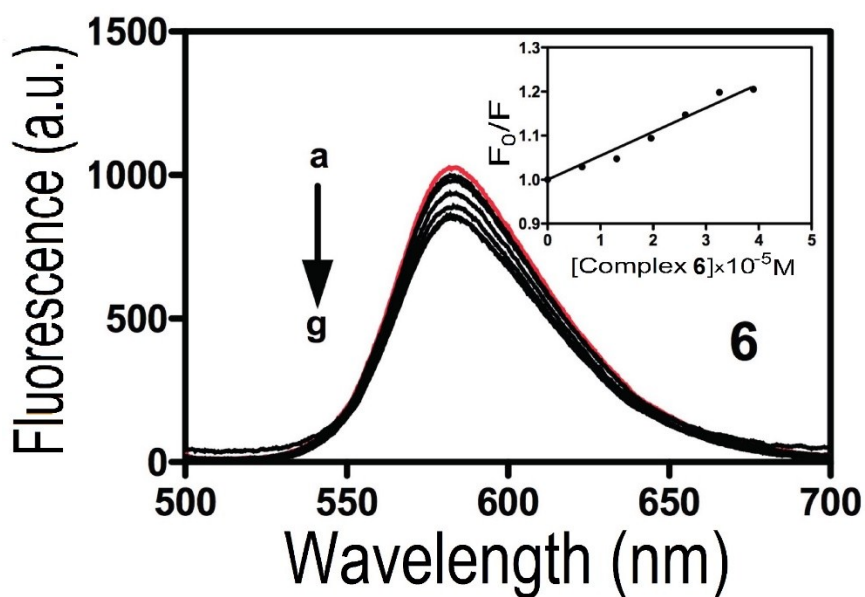
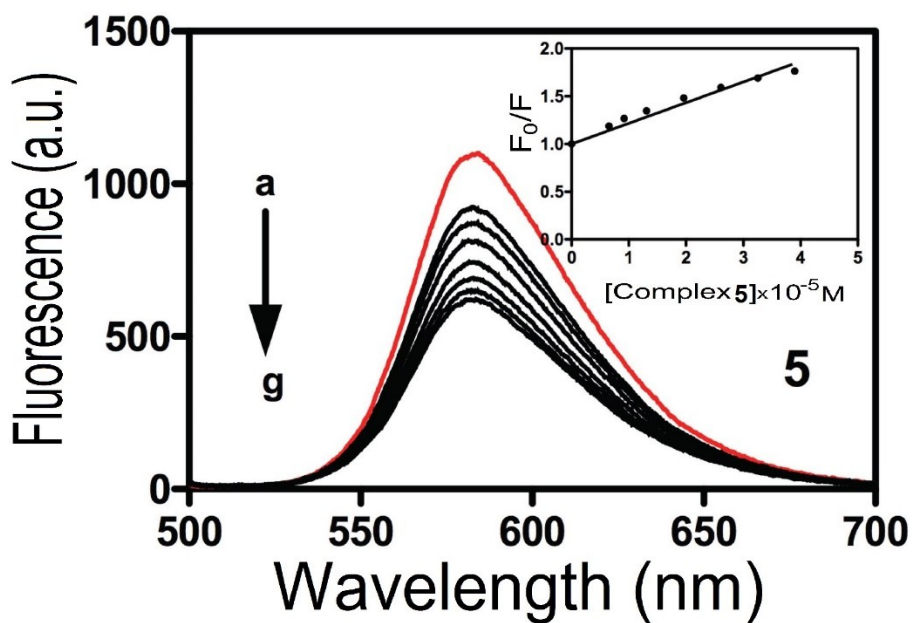
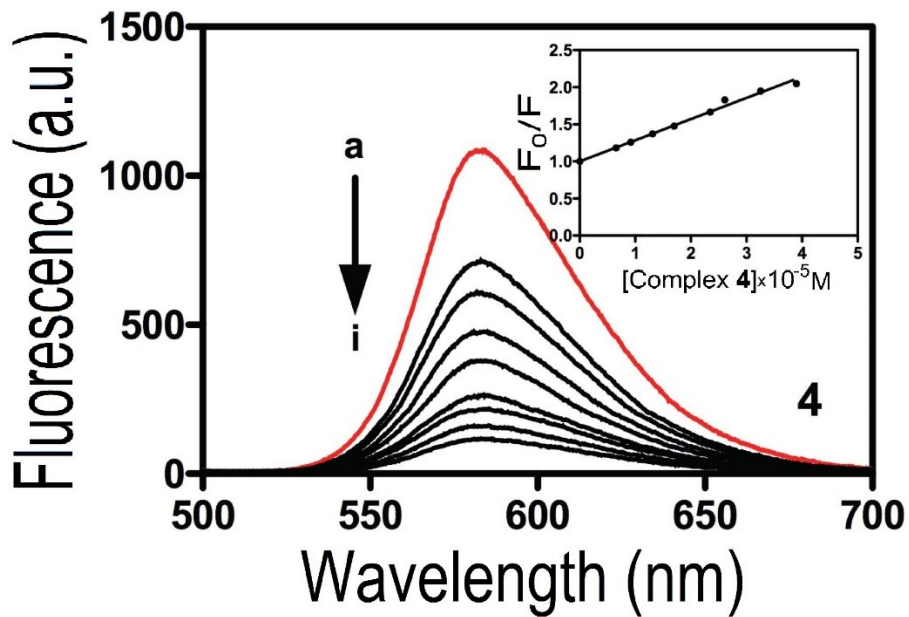


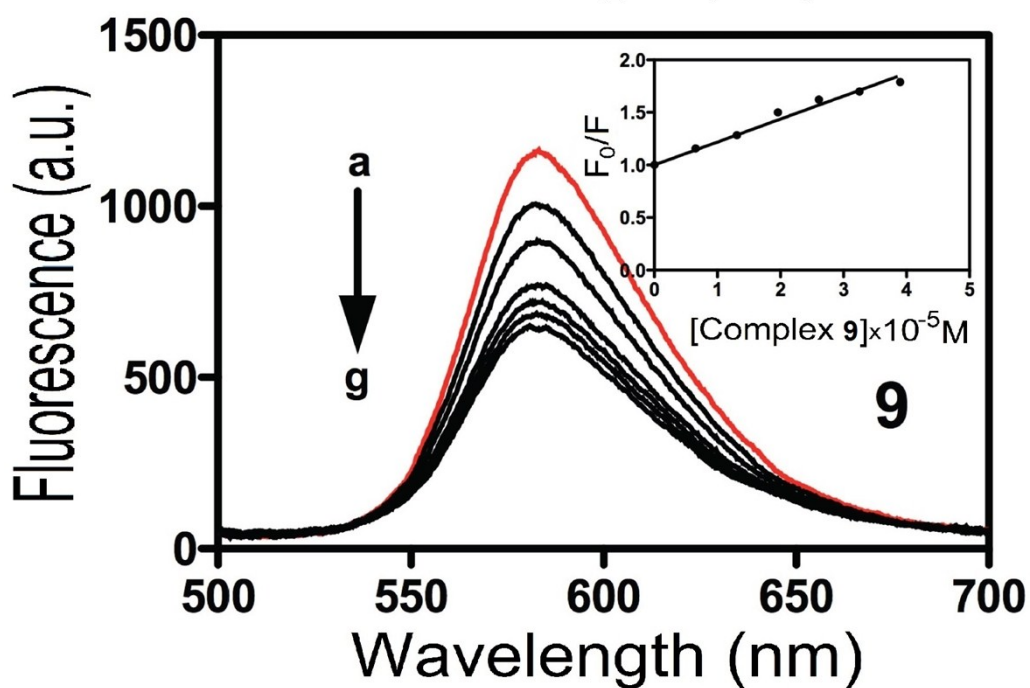
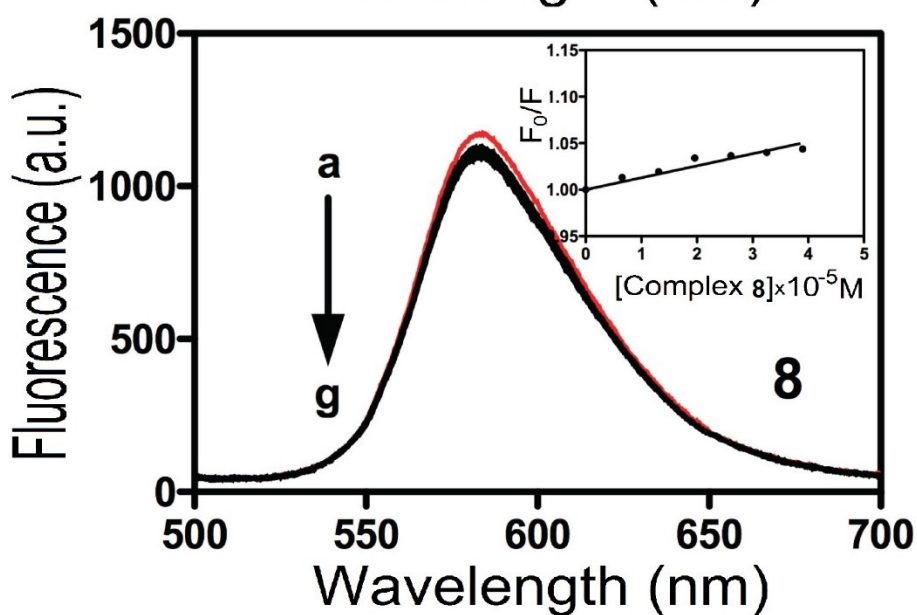
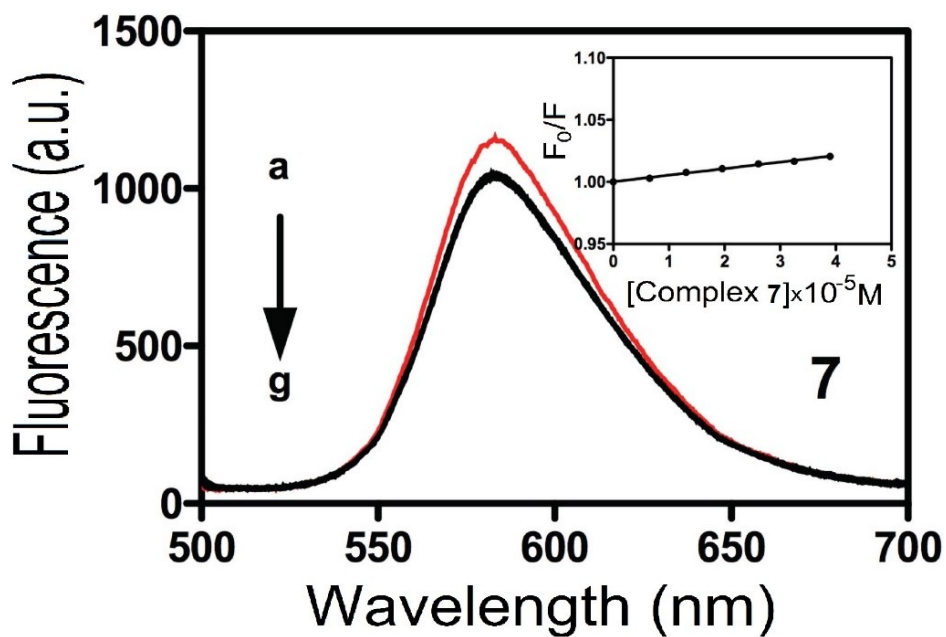


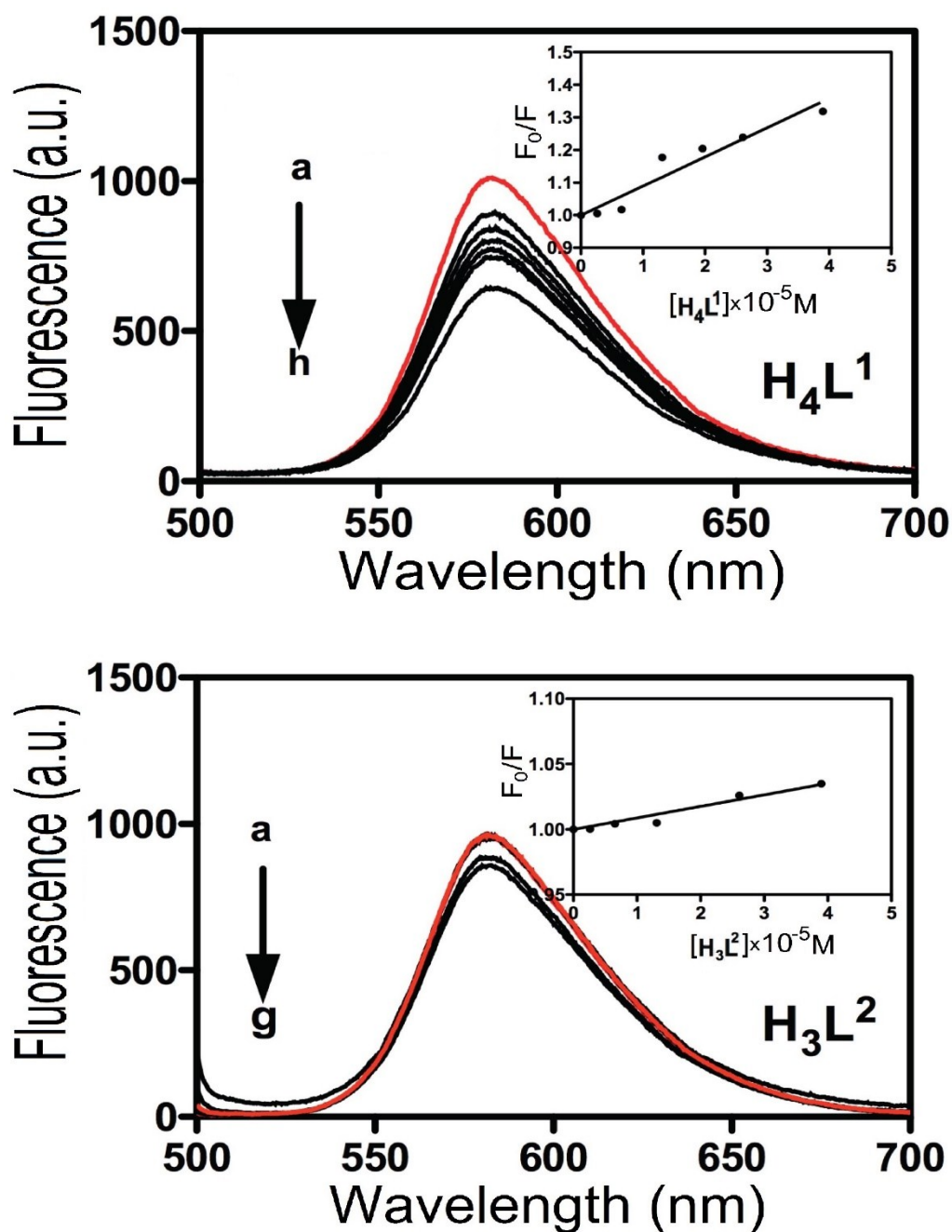
**Figure 22S.** Absorption spectral traces of different complexes (**panel A**) and ligands (**panel B**) in phosphate buffer (10mM, pH 7.2) after gradual addition of calf thymus DNA (from  $a = 0$  to  $h = 24$  mM). Inset shows the plot of  $[DNA]/\epsilon_a - \epsilon_f$  vs.  $[DNA]$  (equation 1).





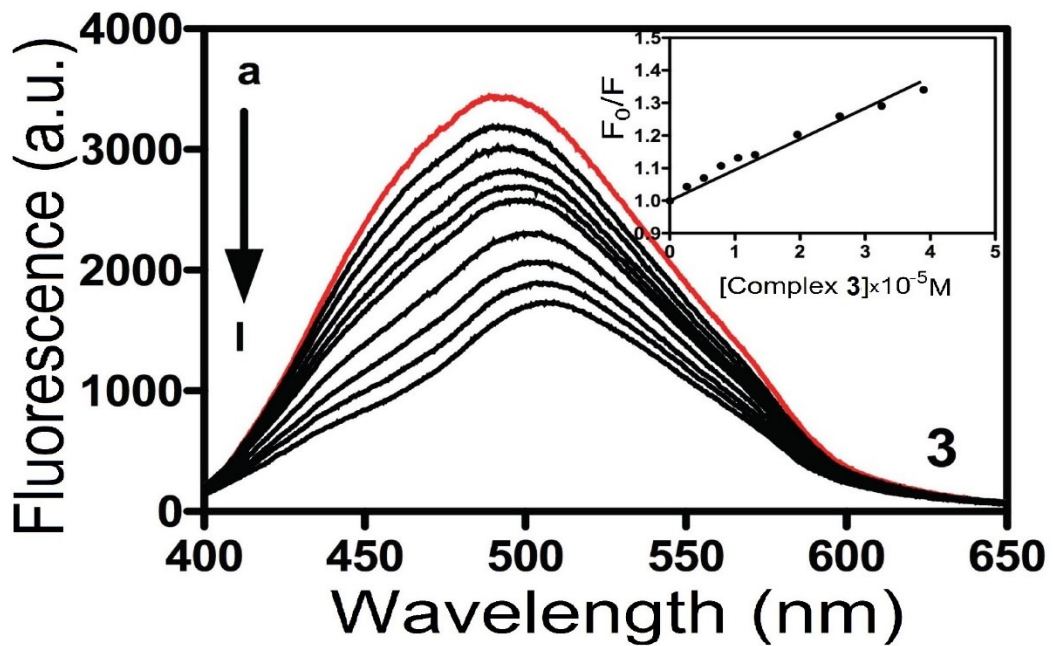
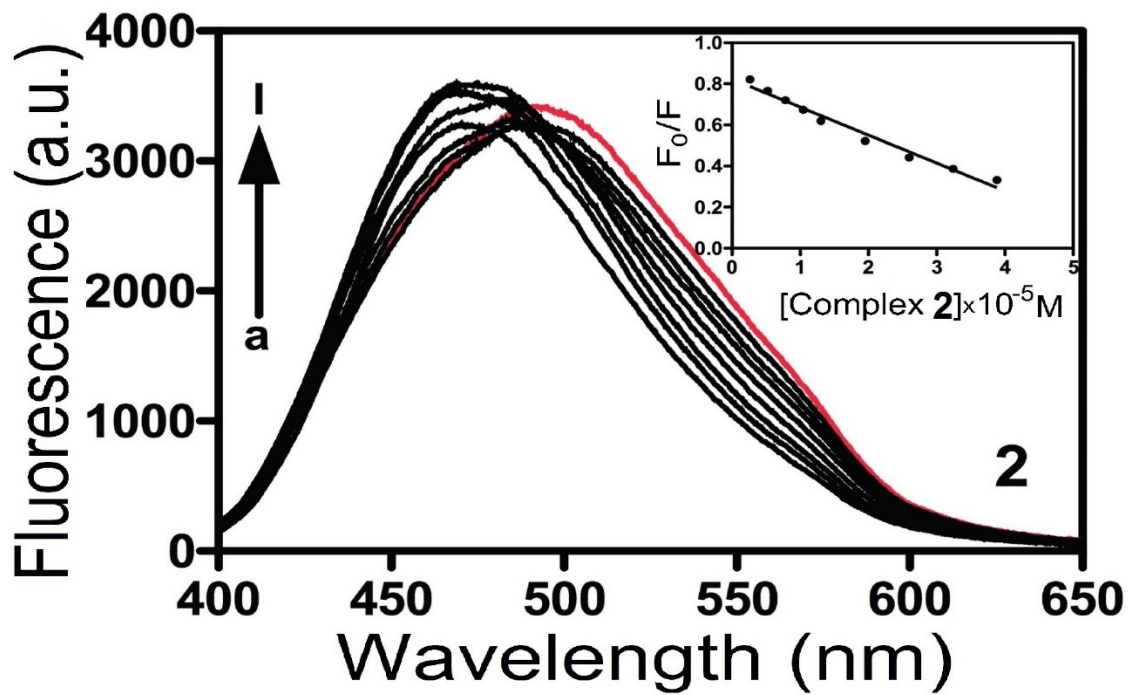
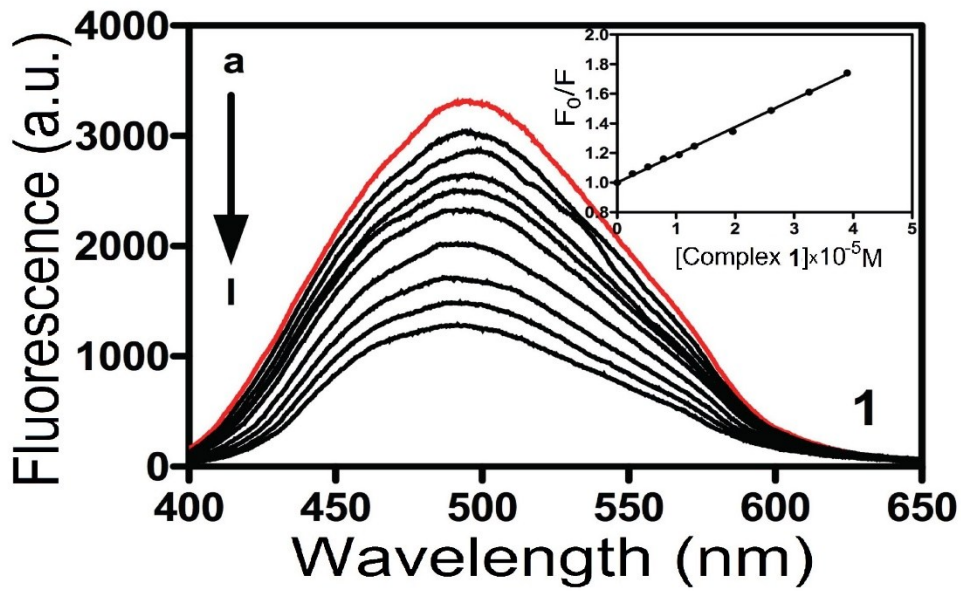


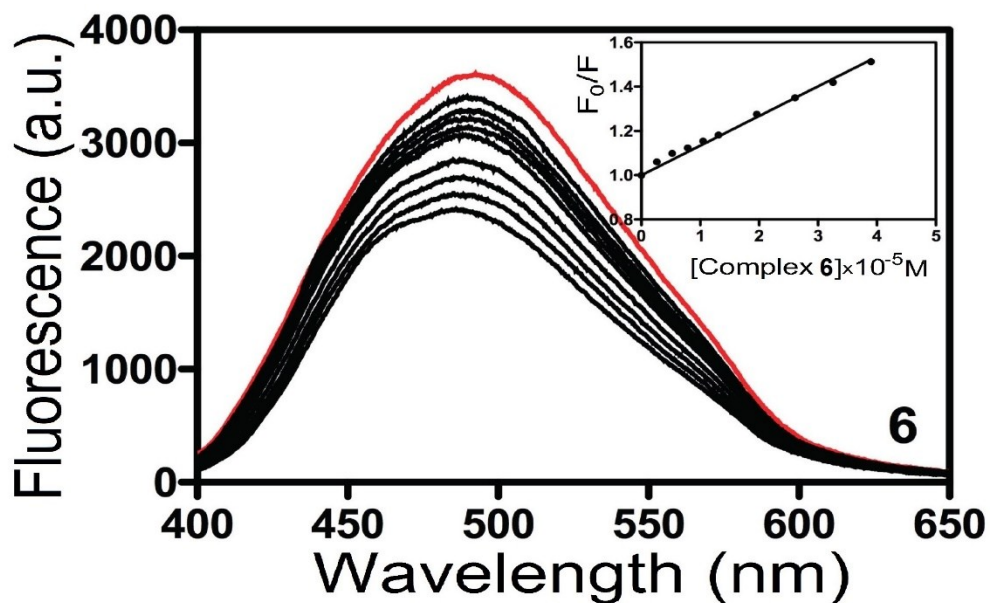
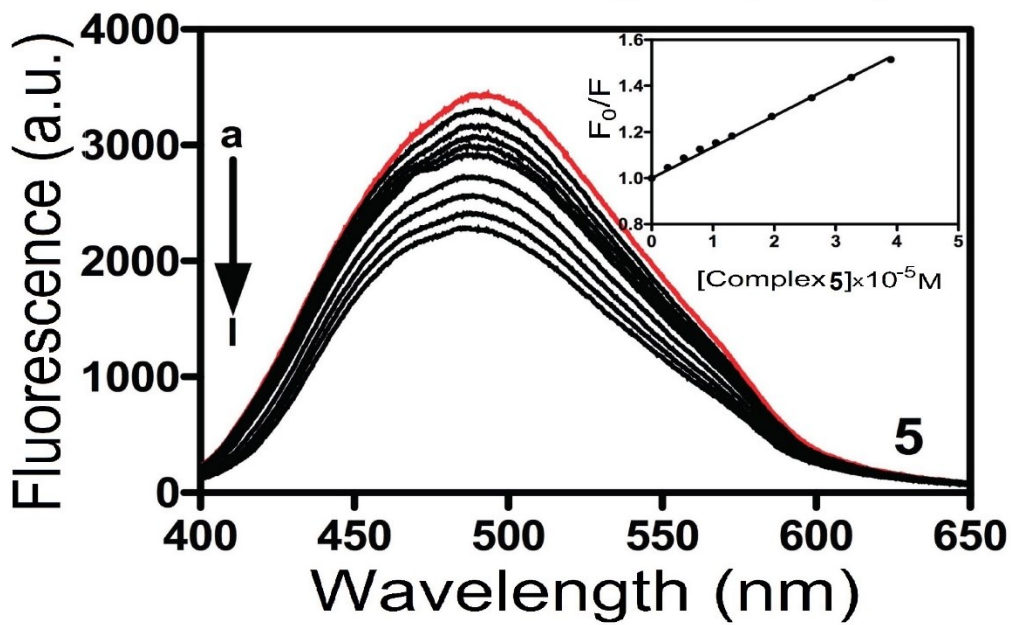
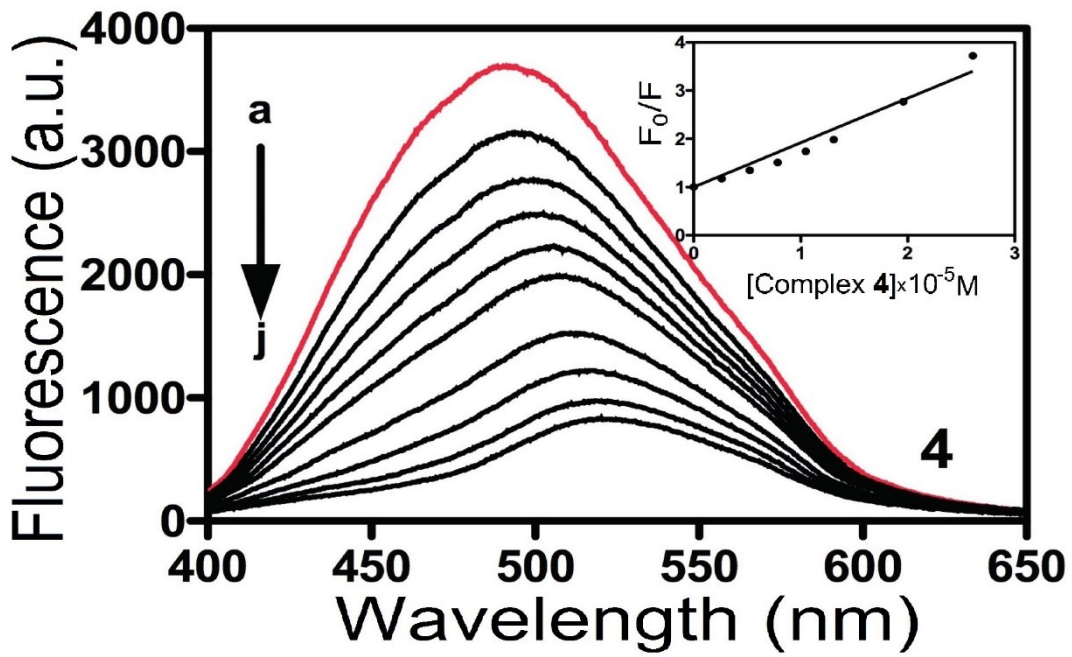


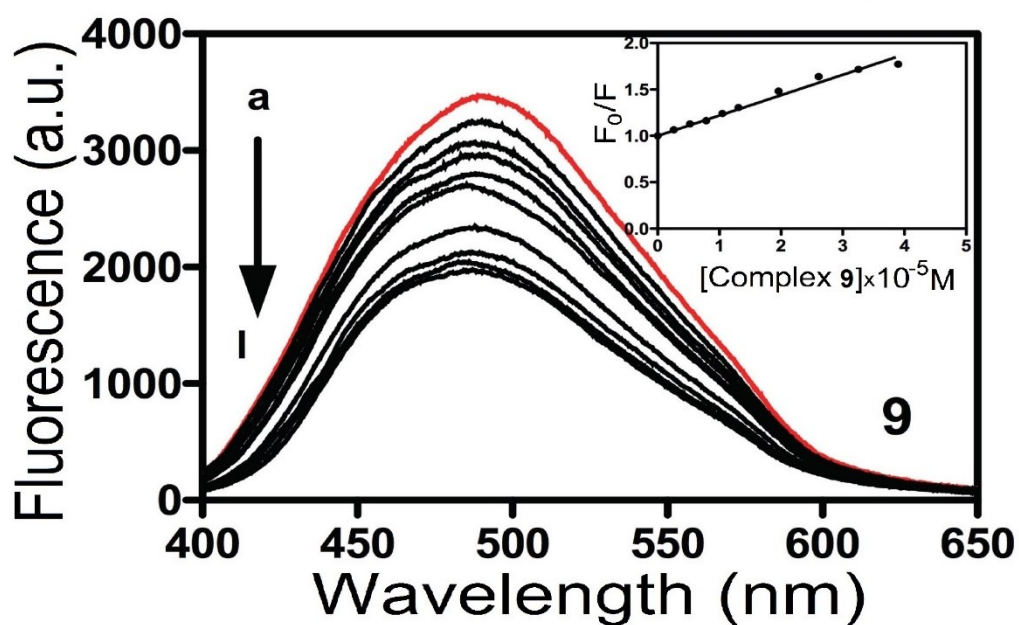
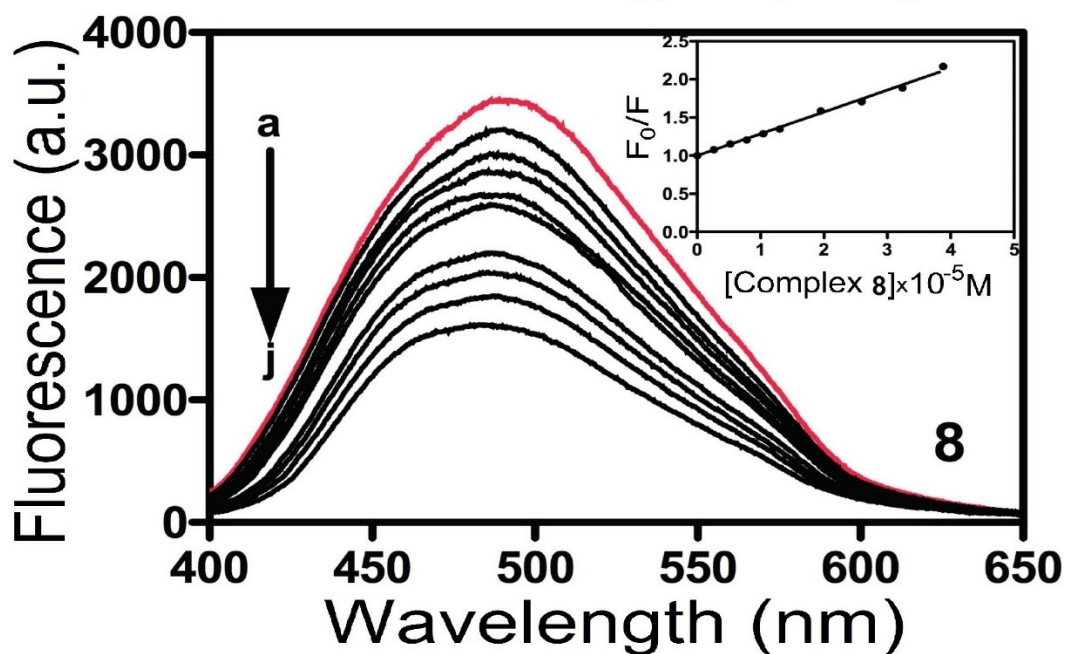
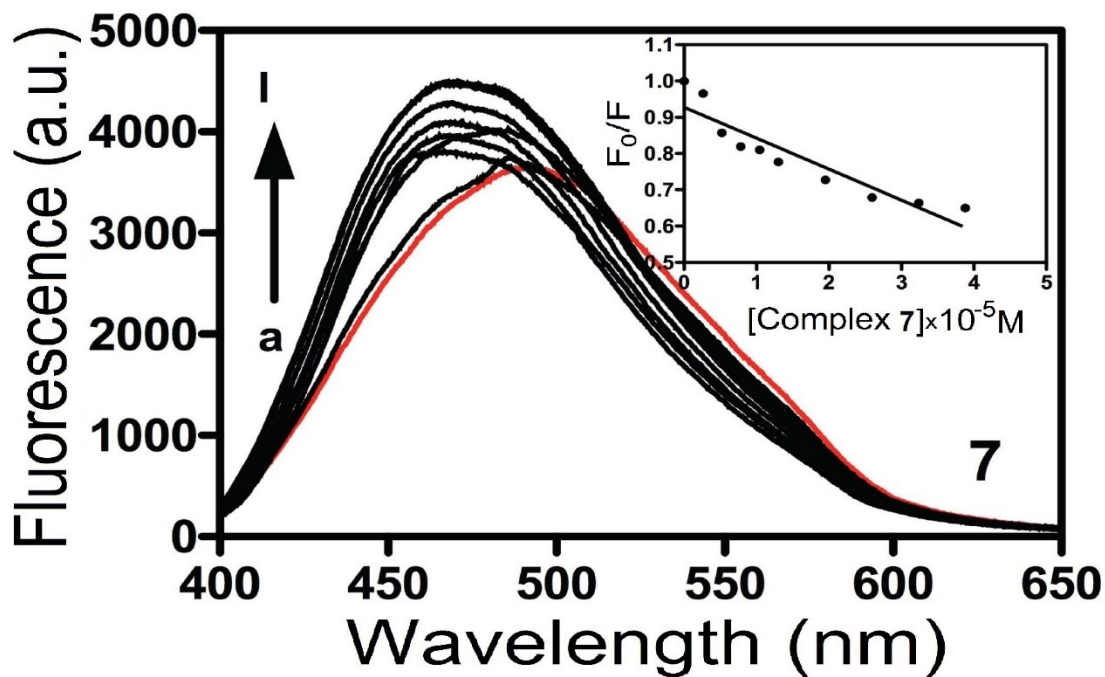


**Figure 23S.** Emission spectra of EB bound to ct-DNA upon excitation at 490 nm in the presence of increasing concentration of different complexes from (a) 0 to (g) 39  $\mu M$ ; ( $[EB] = 6 \mu M$ ,  $[ct-DNA] = 50 \mu M$ ). Inset: Stern Volmer plot of  $F_0/F$  vs.  $[complex]$  for the titration of the complexes to EB-ct-DNA complex.

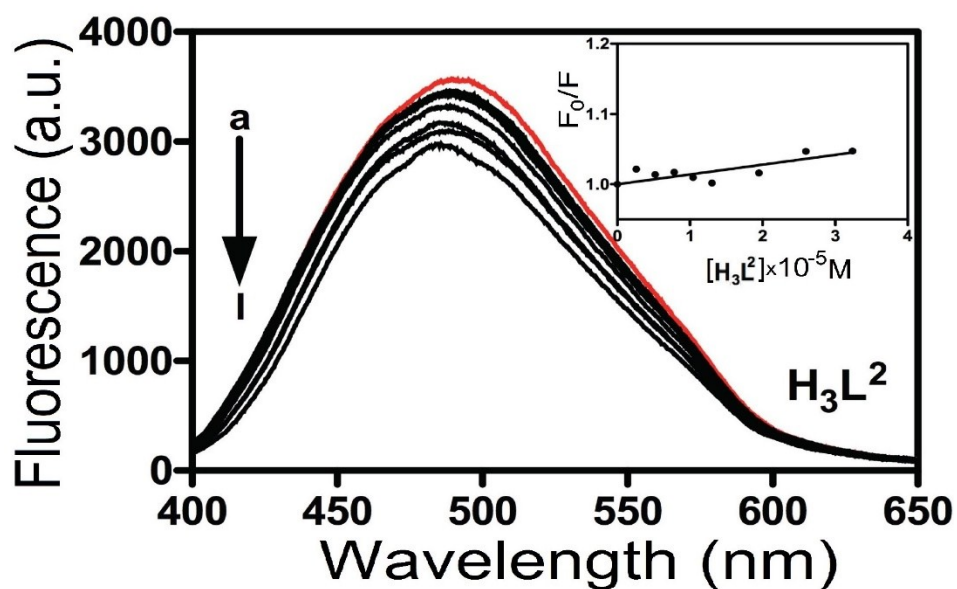
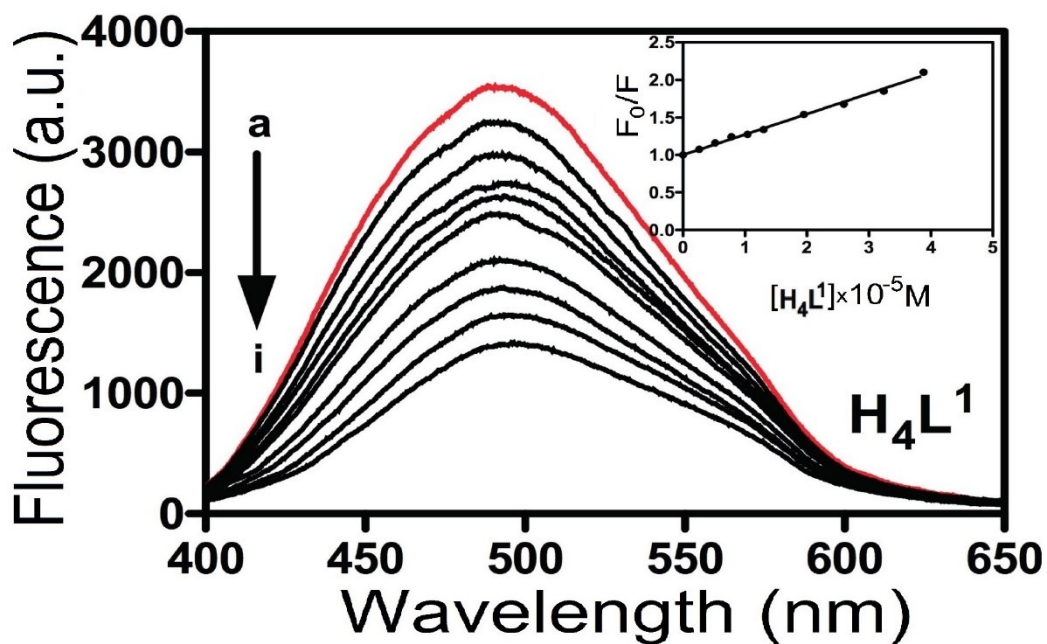






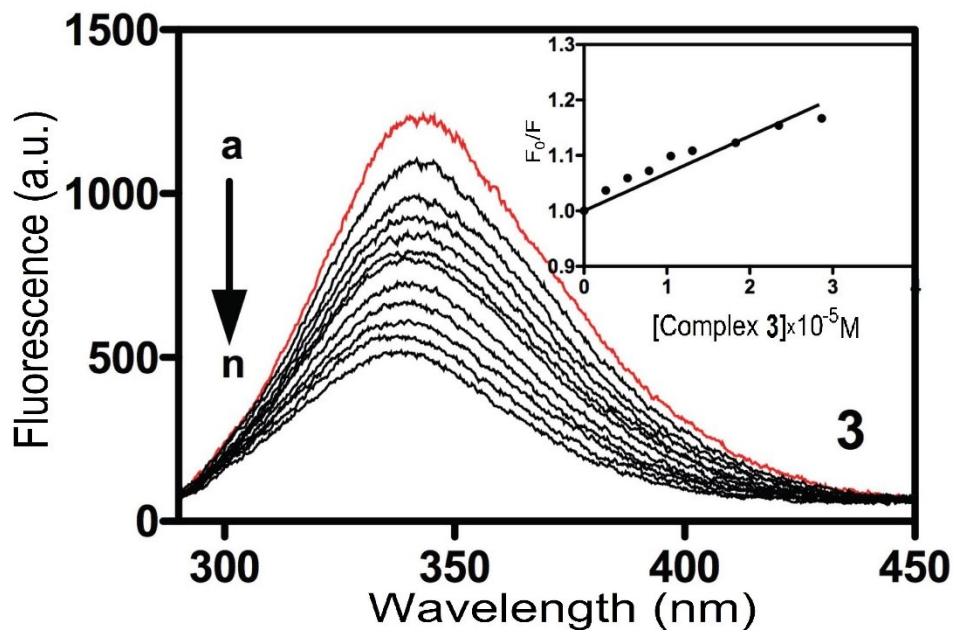
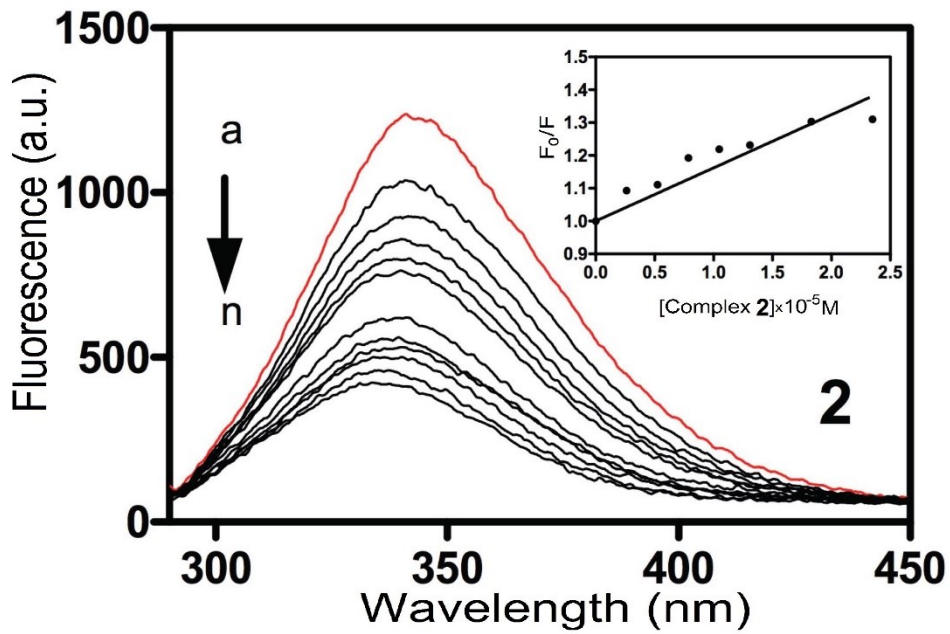
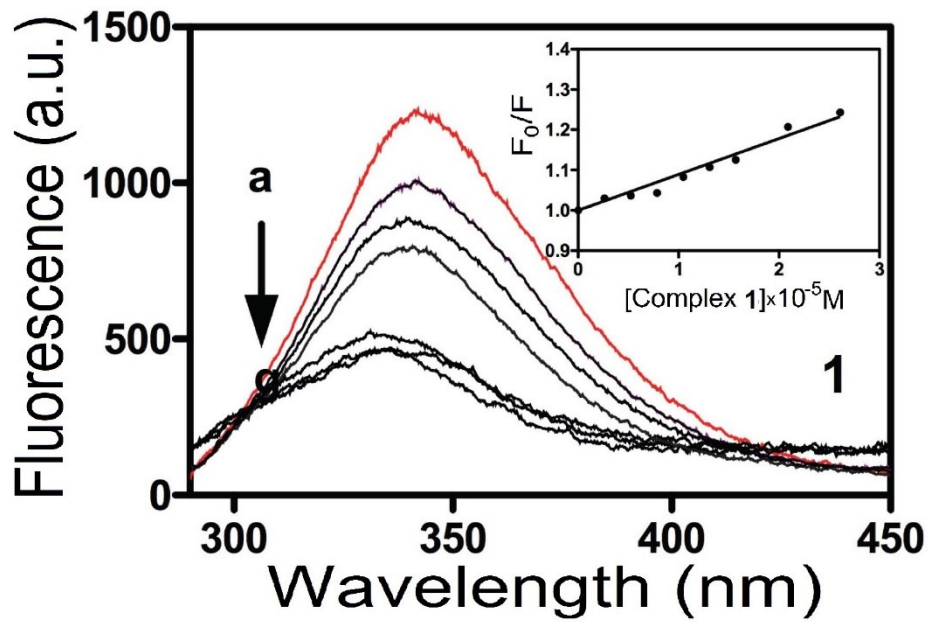


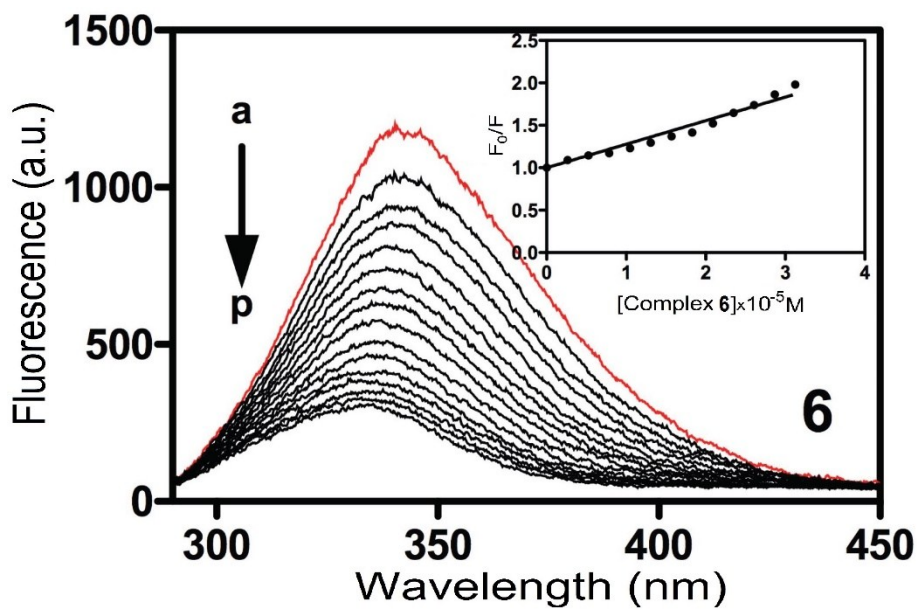
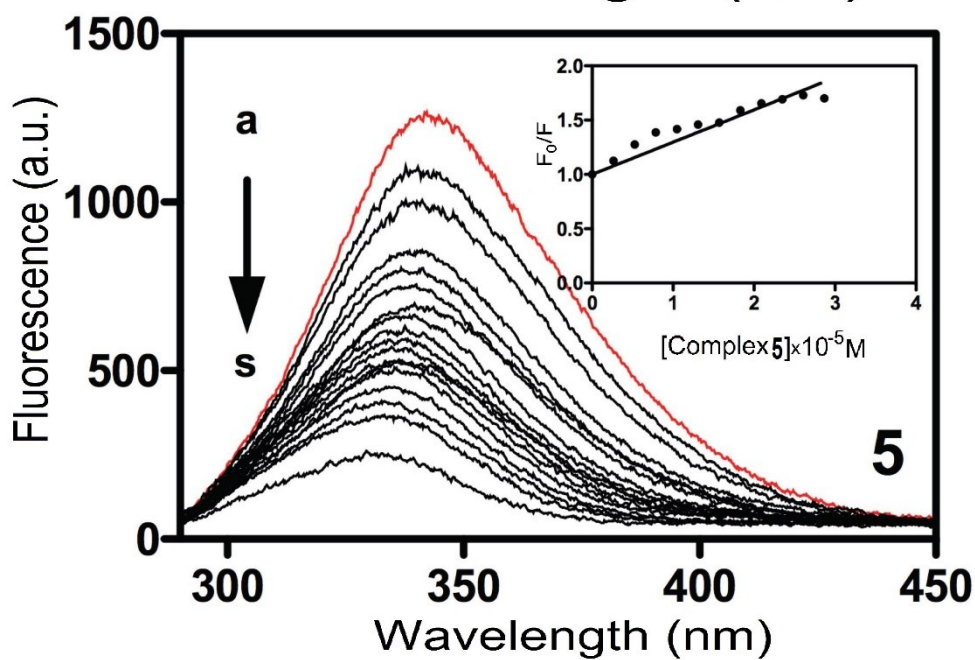
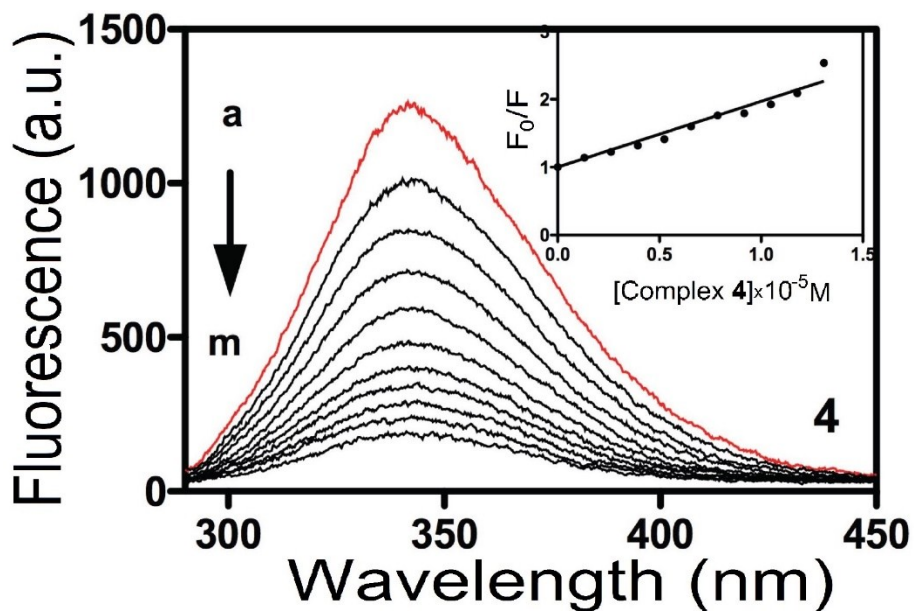


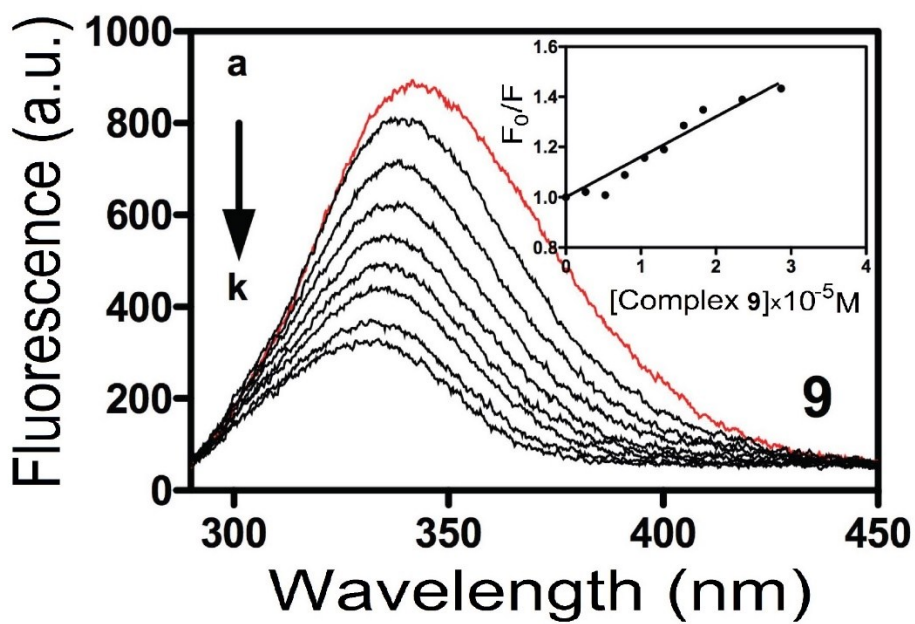
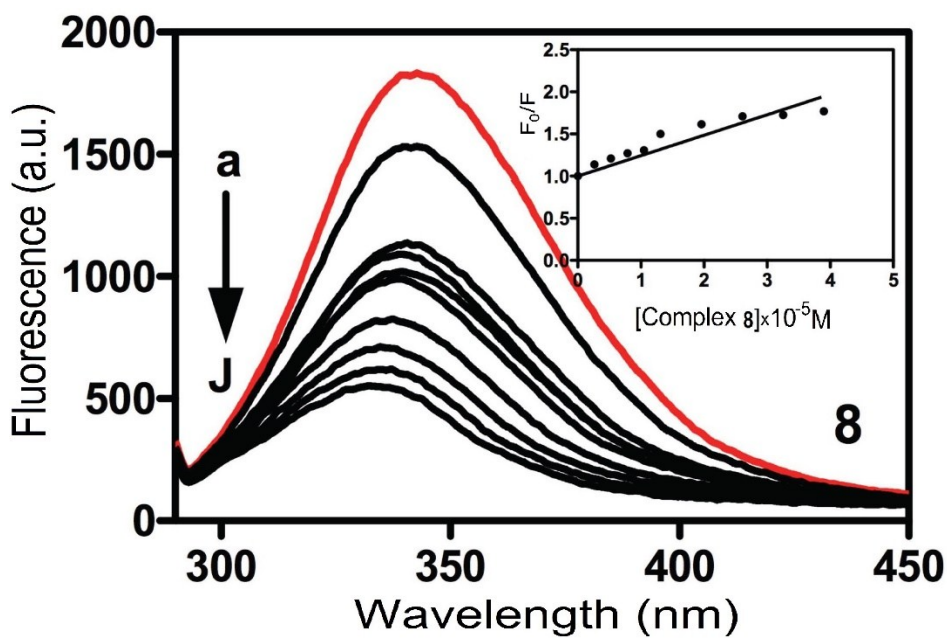
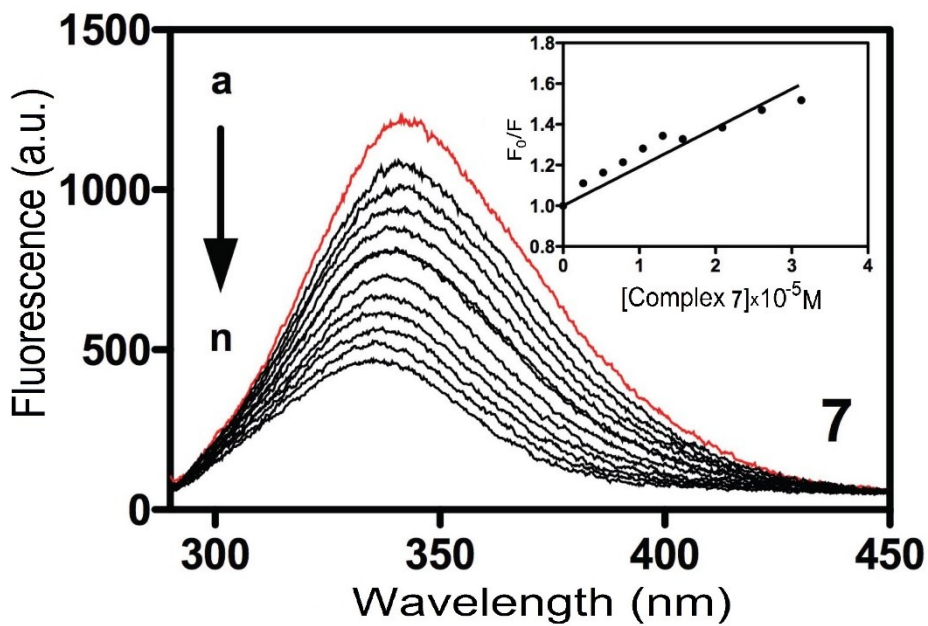


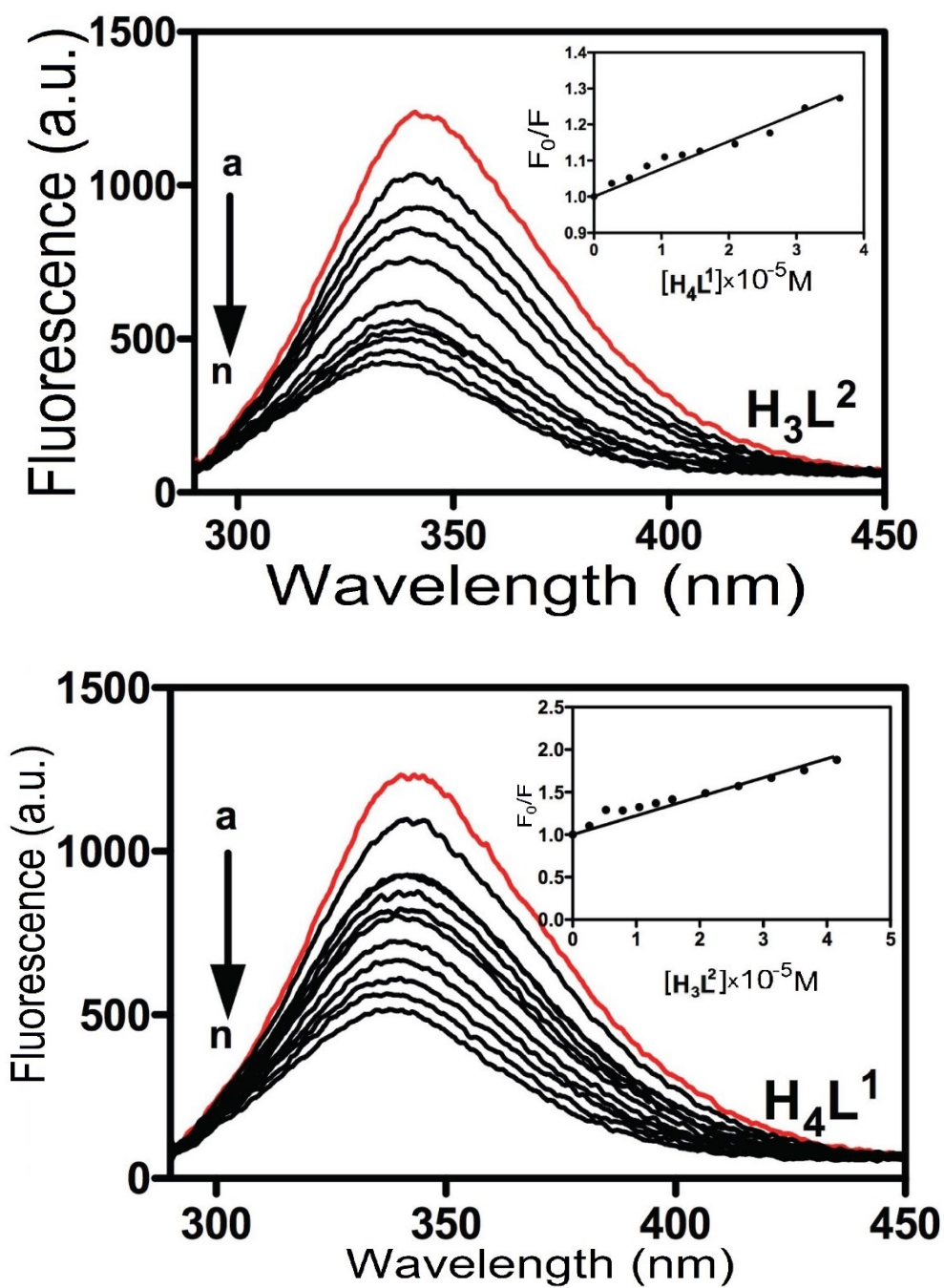
**Figure 24S.** Emission fluorescence spectra of DAPI-ct-DNA complex upon excitation at 338 nm in the presence of increasing concentration of different compounds and proligands in the range 0-36  $\mu$ M. Experiments were performed in 10 mM phosphate buffer, pH 7.2. Inset: Stern-Volmer plot of  $F_0/F$  vs. [complex] for the titration of the complexes to DAPI-ct-DNA complex











**Figure 25S.** Fluorescence emission spectra of BSA upon excitation at 280 nm, in the absence and presence of different concentrations of compounds and proligands. Inset, Stern-Volmer plots of  $F_0/F$  vs. [complex 4] for the titration of the complexes to BSA.